EXPERIMENTAL INVESTIGATION OF TH~ GEOMETRICAL PARAMETERS ON THE PERFORMCE OF SAVONIUS VERTICAL AXIS WIND TURBINE

A THESIS SUBMITTED TO THE GRADUATE
SCHOOL OF APPLIED SCIENCES
OF
NEAR EAST UNIVERSITY

By
Moktar A. Hachem Mohamad

In Partial Fulfillment of the Requirements for
the Degree of Master of Science
in
Mechanical Engineering

NICOSIA, 2016

Moktar A. H. Mohamad : Experimental Investigation of the Geometrical Parameters on the Performance of Savonius Vertical Axis Wind Turbine.

Approval of Director of Graduate School of Applied Sciences

Prof. Dr. İlkay SALİHOĞLU

We certify this thesis is satisfactory for the award of the degree of Masters of Science in Mechanical Engineering

Examining Committee in Charge:

Prof. Dr. Nuri Kayansayan	Committee Chairman, Mechanical Engineering Department, NEU
Assist. Prof. Dr. Elbrus B. Imanov	Computer Engineering Department, NEU
Assist. Prof. Dr. Hüseyin Çamur	Supervisor, Mechanical Engineering Department, NEU

I hereby declare that all information in this document has been obtained and presented in accordance with academic rules and ethical conduct. I also declare that, as required by these rules and conduct, I have fully cited and referenced all material and results that are not original to this work.

Name, Last name: Moktar Mohamad

::~lure; c; | 2- | 2-b 16q

ACKNOWLEDGEMENT

Firstly, I would like to express my thankfulness and gratitude to my country Libya for the financial support during my research. Without that, I was not able to work and search here in Northem Cyprus,

I am greatly indebted to my supervisor Assist. Prof. Dr. Hüseyin Çamur. I am extremely grateful for his support, invaluable guidance and for his continuing help even before I became his student. I also wish to thank him for providing a wonderful work atmosphere and facilities.

J am also grateful to Mr. Youssef Kassem for his valuable suggestions and help. I acknowledge the efficient support of him concerning all experimental measurements.

I always feel lucky to be with so many excellent researchers. Thanks are due to all colleagues of my institute, who were always quite helpful during my stay.

Finally, my sincere thanks go to my parents and my wife who offered her invaluable support to help me during this long educationaljourney.

Thank you for all unconditional support with my studies ....

ABSTRACT

The wind turbine is a technology which converting wind energy to mechanical power or electrical power. Wind energy is easily accessible anywhere in the world and is one of renewable energy. However, in Northern Cyprus, the lower average wind speed become one of the factors wind turbines has not been used widely as an alternative method for generating the electric power. Thereby, small scale Savonius wind turbine which can generate mechanical or electric power in low wind speed must be developed. In this study, different types of Savonius vertical axis wind turbine rotor have been studied, and its performances were investigated. From the study, found that although low wind speed, wind turbine still can perform its function and generate mechanical power. It proves that wind turbines can be as an alternative technology to generate the mechanical or electric power in Turkey especially in Northern Cyprus.

Keyword: Savonius, wind turbine, mechanical power, alternative technology, Northern Cyprus, low wind speed, electric power

ÖZET

Rüzgar türbini rüzgar gücünü mekanik enerjiye veya elektrik enerjisine dönüştüren bir teknolojidir. Rüzgar enerjisi dünyanın her yerinde kolaylıkla erişilebilir ve yenilenebilir enerjilerden biridir. Ancak, Kuzey Kıbrıs'ta düşük rüzgar hızı ortalaması, rüzgar türbinlerinin elektrik enerjisi üretmek için alternatif bir yöntem olarak yaygın bir şekilde kullanılmasını engelleyen etkenlerden biri olmuştur. Dolayısıyla, düşük rüzgar hızında mekanik veya elektrik enerjisi üretebilen küçük ölçekli Savonius rüzgar türbini geliştirilmelidir. Bu çalışmada farklı tür Savonius dikey eksen rüzgar türbini rotoru çalışılmış ve performansları incelenmiştir. Çalışmanın sonucunda düşük rüzgar hızına rağmen rüzgar türbininin görevini yerine getirdiği ve mekanik enerji ürettiği bulunmuştur. Bu, rüzgar türbinin Türkiye'de ve özellikle Kuzey Kıbrıs'ta mekanik veya elektrik enerjisini üretmek için alternatif teknoloji olarak kullanılabileceğini kanıtlamaktadır.

Anahtar Kelimeler: Savonius, rüzgar türbini, mekanik güç, alternatif teknoloji, Kuzey Kıbrıs, Düşük rüzgar hızı, elektrik gücü

TABLE OF CONTENTS

LIST OF TABLES

LIST OF FIGURES

LIST OF SYMBOLS USED

A	Swept Area
Ap	Plan form Area
Ar	Aspect Ratio
C	Chord Length
Co	Drag Coefficient
Co.0	Drag Coefficient at Zero Lift
Co;ı	Induced Drag Coefficient
Cr	Friction Coefficient
C1	Lift Coefficient
Cr	Torque Coefficient
CP	Power Coefficient
Fo	Drag Force
F1	Lift Force
n	Rotational Speed in Evolutions per Second
Pm	Mechanical Power
Pw	Extracted Power from the Wind
Re	Reynolds Number
V	Wind Velocity
Vrotor	Velocity of Rotor
V00	Wind Speed without Rotor Interruption
Vr	Rotor Velocity
V_T«	Relative Velocity
Vw	Wind Velocity
p	Air Density
T	Actual Torque
Tm	Mechanical Torque
Tw	Wind Torque
00	Angular Velocity
SRC	Specific Rated Capacity

N	Kinematic Viscosity
8	Boundary Layer Thickness

CHAPTERl

INTRODUCTION

1.1 Background of the Study

Energy has always been the most important asset for the ~c;cmomy 'and social growth development of a country. It is no longer viewed as affluence as it used to be but it has become a compulsion in our everyday life.

The conventional energy sources are limited and pollute the environment. So more.attention and interest have been paid to the utilization of renewable energy source such as Wind Energy, Fuel Cell, Solar Energy etc. Wind Energy is the fastest growing and most promising renewable energy source among them as it is economically viable.

Nowadays, the wind energy is one of the most important sources of clean energy available. The generation of electricity by converting this type of energy has become increasingly important in recent years. The term wind energy itself describes its process by which the wind is used to generate mechanical power which then able to generate electricity. Wind turbines convert the kinetic energy from the wind into mechanical power. The energy conversion principle of the wind turbine is caused by the effect of the kinetic energy from the air flow. The energy from the wind is then converted into rotational energy by the wind turbine rotor. The conversion can be made either by aerodynamic forces or the air pressures which are acting on the rotor blades. Afterwards, the rotational energies produced are converted into electrical energy via a generator to be utilized for mechanical work.

There are so many types of wind turbines that are currently being used to generate electricity, such as horizontal axis wind turbines (HAWT) and vertical axis wind turbines (VAWT) where both types of turbines depend on the orientation of their axis of revolution. HAWT has the main rotor shaft and electrical generator at the summit of a tugboat, and may be placed inward or out of the current air movement. Small turbines are pictured by a simple wind vane, while large turbines generally use a wind sensor coupled with a servo motor. Most of them have a gearbox which runs around the slow rotations of the blades into quicker rotations that is more suitable to drive an electric generator. VAWT is also known as a crosswind axis machine. In this machine, the axis of rotation is perpendicular to the direction of the wind. VAWT is generally not self-starting and has a low power coefficient.

In this work different geometries of Savonius wind turbine are experimentally studied in order to determine the most effective operation parameters. Additionally, it describes the design of different kinds of Savonius vertical axis wind turbine rotors having different number .of blades and blade size. In the present research; various geometry parameters of Savoniusrotors including number of blades, blade size, and overlap ratio are studied experimentally. The aim of this work is to determine the optimum configuration of the Savonius rotor which gives the higher performance. Also, it is to study the influence of the different designs on rotational speed and power of rotor in different wind speed. Various geometries of Savonius rotors are studied experimentally and theoretically based on velocity analysis in order to predict the average power of the Savonius wind turbine in different dimensions

1.2 **Objective** of the **Research**

The aims of this project are as follows:

i. To study the performances of two different types of Savonius vertical axis wind turbine blade rotors.

ii. To study the effects of'the size of the rotor on the performances of Savonius wind turbine rotors.

iii. Compare the experimental result, from previous research outcomes, with the empirical result which obtained by velocity analysis

1.3 Outline of the Thesis

The thesis is presented in the following direction.

i. A brief description of the findings of both experimental and numerical investigations for different models of Savonius wind turbine rotor from previous research outcomes.

ii. Discuss the result yielded from the analyzing the velocity of the Savonius wind turbine.

iii. The final conclusion on the current study, recommendation and guidance based on the laggings for the future investigation.

CHAPTER2

FUNDAMENTALS OF WIND TURBINES

2.1 Power in the Wind

Wind energy is not a constant source of energy. It varies continuously and gives energy in sudden bursts. About 50% of the entire energy is given out in just 15% of the operating time (Prabhuraj et al., 2014). Wind strengths vary and thus cannot guarantee continuous power. It is best used in the context of a system that has a significant reserve capacity, such as hydro, or reserve load, such as a desalination plant, to mitigate the economic effects of resource variability. The total capacity of wind power on this earth that can be harnessed is about 72 TW. There are now many thousands of wind turbines operating in various parts of the world, with utility companies having a total capacity of 59,322 MW (Ravichandrudu and Kumar, 2014).

The power generation of wind energy was about 94.1GW in 2007 which makes up nearly 1% of the total power generated in the world (Ravichandrudu and Kumar, 2014). Globally, the long-term technical potential of wind energy is believed to be 5 times the current global energy consumption or 40 times current electricity demand. This would require covering 12.7% of all land area with wind turbines. This land would have to be covered with 6 large wind turbines per square kilometer (Ravichandrudu and Kumar, 2014; Nag, 2008).

The power extracted from the wind can be calculated by the given formula:

$$P_W = 0.5\, \rho C_p V^3 A \tag{2.1}$$

P_W = extracted power from the wind,

ρ = air density, (approximately 1.225 kg/m^3 at 20°C at sea level)

A = Swept area (in m^2)

V = wind velocity (m/s) (velocity can be controlled between 3 to 30 m/s)

C_p = the power coefficient, which is a function of both tip speed ratio (λ), and blade pitch angle, (β) (Degrees)

Power coefficient (C_p) is defined as the ratio of the output power produced to the power available in the wind (Morshed, 2010).

2.1.1 Betz Limit

No wind turbine could convert more than 59.3%of the kinetic energy of the wind into Mechanical energy turning a rotor. This is known as the Betz Limit, and is the theoretical Maximum coefficient of power for any wind turbine. The maximum value of C_p according to Betz limit is 59.3%. For good turbines it is in the range of 35-45% (Aldo, 2009).

2.2. Types of Wind Energy Conversion Devices

A wind turbine is a rotating machine which converts the kinetic energy in wind into mechanical energy. If the mechanical energy is then converted to electricity, the machine is called a wind generator, wind turbine, wind power unit (WPU), wind energy converter (WEC), or aero generator (Ali, 2013). Wind turbines can be separated into two types based by the axis in which the turbine rotates (Kaldellis, 2010). Turbines that rotate around a horizontal axis are more common. Vertical-axis turbines are less frequently used.

- Horizontal axis wind turbine
    a) Dutch-type" grain grinding windmills.
    b) Multi-blade water-pumping windmills.
    c) High speed propeller type windmills.
- Vertical axis wind turbine
    a) The Savonius rotor.
    b) The Darrieus rotor.

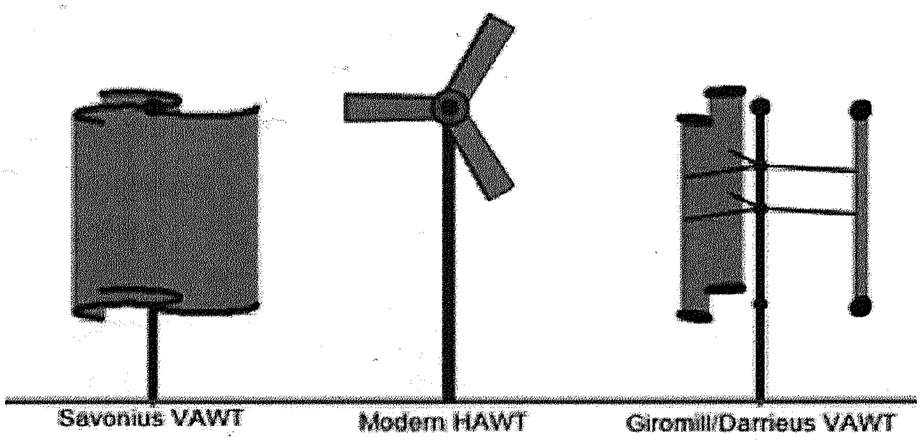

Figure 2.1: Different Wind Turbines

A. Horizontal Axis Wind Turbine

Horizontal-axis wind turbines (HAWT) have the main rotor shaft and electrical generator at the top of a tower, and must be pointed into the wind. Most have a gearbox, which turns the slow rotation of the blades into a quicker rotation that is more suitable to drive an electrical generator. Since a tower produces turbulence'behind it, the turbine is usually pointed upwind of the tower. Turbine blades are made stiff to prevent the blades from being pushed into the tower by high winds. Additionally, the blades are placed a considerable distance in front of the tower and are sometimes tilted up a small amount,

Downwind machines have been built, despite the problem of turbulence, because they don't need an additional mechanism for keeping them in line with the wind, and because in high winds the blades can be allowed to bend which reduces their swept area and thus their wind resistance. Since cyclic (that is repetitive) turbulence may lead to fatigue failures, most HAWTs are upwind machines (Singh, 2008).

High-speed Propeller-Type Wind Machines.

The horizontal-axis wind turbines that are used today for electricity generation don't operate on thrust force, but on the aerodynamic forces that develop when wind flows around a blade of airfoil design. Actually, the windmills that work on thrust forces are less efficient (Singh, 2008).

Airfoil

The wind stream at the top of the airfoil has to traverse a longer path than that at the bottom, leading to a difference in velocities. This gives rise to a difference in pressure (Bernoulli's principle), and a lift force is produced. There is also a drag force that tries to push the aerofoil back in the direction of the wind. The aggregate force is determined by the resultant of these forces (Singh, 2008).

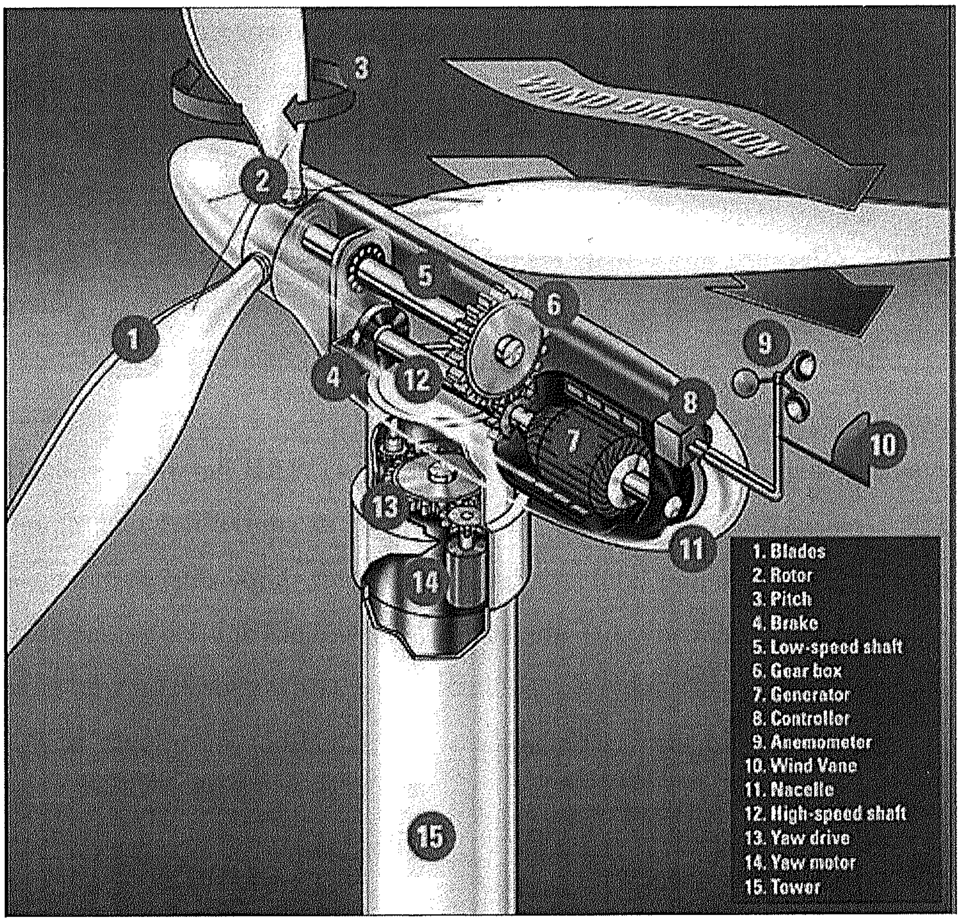

Figure 2.2: Various Parts in a Horizontal Axis Wind Turbine- Propeller Type

Advantages of HAWT:

- Variable blade pitch, which gives the turbine blades the optimum angle of attack. Allowing the angle of attack to be remotely adjusted gives greater control, so the turbine collects the maximum amount of wind energy for the time of day and season.

- The tall tower base allows access, to stronger wind in sites with wind shear. In some wind shear sites, every ten meters up, the wind speed can increase by 20% and the power output by 34%.
- High efficiency, since blades always move perpendicularly to the wind, receiving power through the whole rotation. In contrast, all vertical axis wind turbines, and most proposed airborne wind turbine designs, involve various types of reciprocating actions, requiring airfoil surfaces to backtrack against the wind for part of the cycle. Backtracking against the wind leads to inherently lower efficiency (Singh, 2008).

Disadvantages of HAWT:

- The tall towers and blades up to 90 meters long are difficult to transport. Transportation can now cost 20% of equipment costs.
- Tall HAWTs are difficult to install, needing very tall and expensive cranes and skilled operators.
- A massive tower construction is required to support the heavy blades, gearbox, and generator.
- Reflections from tall HAWTs may affect side lobes of radar installations, creating signal clutter, although filtering can suppress it.
- Downwind variants suffer from fatigue and structural failure caused by turbulence when a blade passes through the tower's wind shadow (for this reason, the majority of HAWTs uses an upwind design, with the rotor facing the wind in front of the tower).
- HAWTs require an additional yaw control mechanism to turn the blades toward the wind.

B. **Vertical** Axis **Wind Turbine**

Vertical-axis wind turbines (or VAWTs) have the main rotor shaft arranged vertically. Key advantages of this arrangement are that the turbine does not need to be pointed into the wind to be effective. This is an advantage on sites where the wind direction is highly variable. VAWTs can utilize winds from varying directions. With a vertical axis, the generator and gearbox can be placed near the ground, so the tower doesn't need to support it, and it is more accessible for maintenance. The drawbacks are that some designs produce pulsating torque. Drag may be created when the blade rotates into the wind (Singh, 2008).

1. Savonius Rotor.

The Savonius rotor is an extremely simple vertical- axis device that's entirely because of the thrust force of the wind. The basic .equipment is a drum cut into two halves vertically. The two parts are attached to the two opposite sides of a vertical shaft. The wind blowing into the assembly meets two different surfaces- convex and concave- and different forces are exerted on them, giving torque to the rotor (Singh, 2008).

Providing a certain overlap between drums increases the torque because the wind blowing on the concave side turns around and pushes the inner surface of the other drum, which partly cancels the wind thrust on the convex side. An overlap of one- third of the drum diameter gives the best results (Singh, 2008).

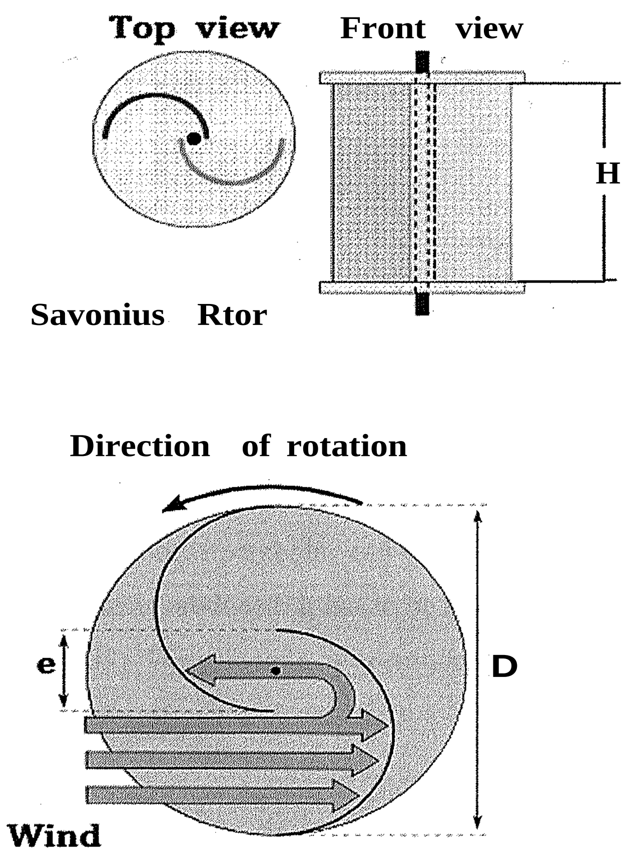

Figure 2.3: The Savonius Rotor

2. Darrieus Rotor

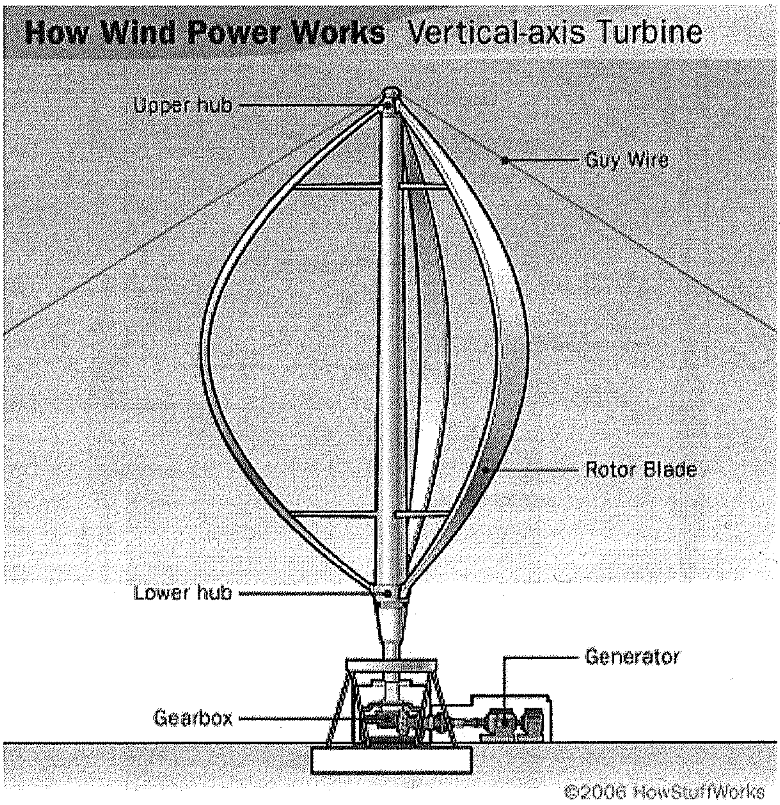

Figure 2.4: Darrieus Wind Turbine

In a Darrieus rotor, two or more flexible blades are attached are attached to a vertical shaft. The blades, bow outward taking the shape of a parabola, and are of a symmetrical airfoil section. When the rotor is stationary no torque is produced. It has to be started by some external means as it has no starting torque (Singh, 2008). The principle of operation is given in the figure.

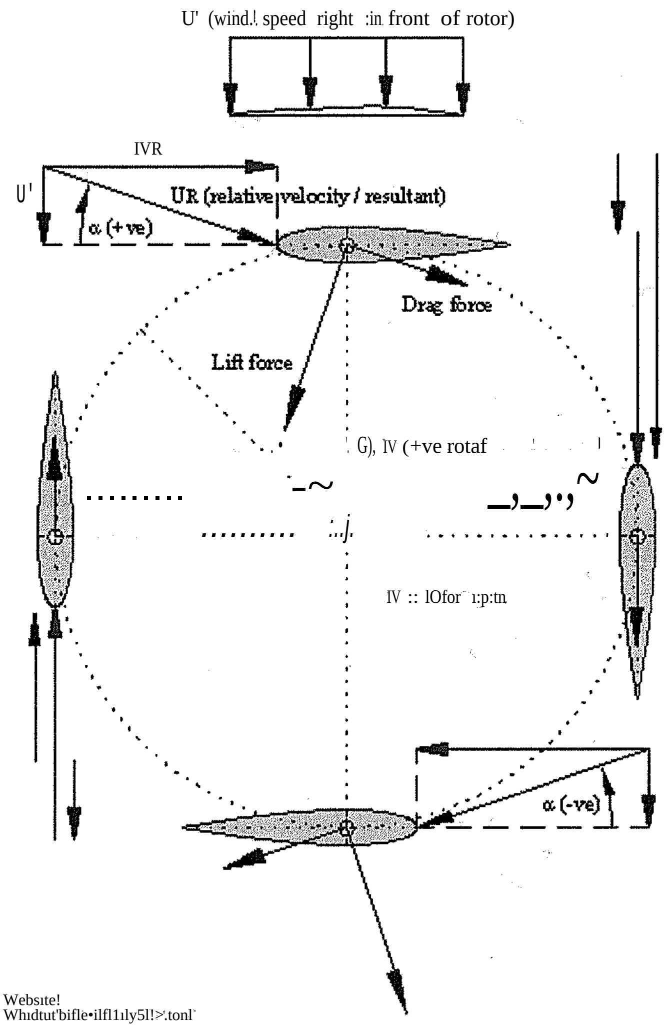

Figure 2.5: Forces Acting on a Blade of the Darrieus Rotor

At each position the lift force has a positive component in the direction of rotation, giving rise to a net positive torque. The torque is different in different directions. It varies from zero to maximum in about a quarter of a revolution. The torque makes two complete excursions from zero to maximum and back in each revolution-both in a positive sense. The pulsations in the shaft torque can be minimized by using a three blade system. However, the two blade design has a lower erection cost (Singh, 2008).

The torque here is a function of speed of rotation and the wind speed. The torque increases with rotational speed, and is zero at zero rotational speed. Torque increases with wind speed up to a certain value and then falls off at very high wind speeds. Therefore, this has inbuilt protection from stormy weather- the rotor tends to stall at high winds (Singh, 2008).

As the Darrieus rotor operates on the lift force, its efficiency approaches that of modem horizontal- axis propeller-type windmills. The theoretical limit of power extraction can be shown to be 0.554 times the power in the wind; the corresponding Betz limit for a horizontal-axis machine is 0.593.

The Darrieus rotor, with its efficiency and high speed, is perfectly suited for electrical power generation. The cost of construction is low because the generator and the gear assembly can be located at the ground level, drastically reducing the cost of the tower. However, it is unable to take advantage of the wind speeds available at the higher altitudes.

An electrical machine provides the starting torque running as a motor, but changing to generating mode as the rotor starts generating power.

Advantages of VAWT

- A massive tower structure is less frequently used, as VAWTs are more frequently mounted with the lower bearing mounted near the 'ground.
- Designs without yaw mechanisms are possible with fixed pitch rotor designs.
- A VAWT can be located nearer the ground, making it easier to maintain the moving parts.
- VAWTs have lower wind start-up speeds than HAWTs. Typically, they start creating electricity at 6 M.P.H. (10 km/h).
- VAWTs may have a lower noise signature.

Disadvantages ofVAWT

- Most VAWTs produce energy at only 50% of the efficiency of HAWTs in large part because of the additional drag that they have as their blades rotate into the wind.
- While VAWTs' parts are located on the ground, they are also located under the weight of the structure above it, which can make changing out parts nearly impossible without dismantling the structure if not designed properly.

- Having rotors located close to the ground where wind speeds are lower due to wind shear, VAWTs may not produce as much energy at a given site as a HAWT with the same footprint or height.
- Because VAWTs are not commonly deployed due mainly to the serious disadvantages mentioned above, they appear novel to those not familiar with the wind industry. This has often made them the subject of wild claims and investment scams over the last 50 years (Singh, 2008).

2.3 **Some Relevant Definitions**

Solidity:

The solidity of a wind rotor is the ratio of the projected blade area to the area of the wind intercepted. The projected blade area does not mean the actual blade area; it is the blade area met by the wind or projected in the direction of the wind.

The solidity of the Savonius rotor is natural unity, as the wind sees no free passage through it. For a multiple blade water-pumping windmill, it is typically around 0.7. For high-speed horizontal axis machines, it lies between 0.01 and 0.1; for the Darrieus rotor also it is of the same order.

Solidity has a direct relationship with the torque and speed. High-solidity rotors have high torque and low speed, and are suitable for pumping water. Low-solidity rotors, on the other hand, have high speed and low-torque, and are typically suited for electrical power generation (Diaz et al., 1991).

Tip Speed Ratio:

The tip speed ratio (TSR) of a wind turbine is defined as

$$\lambda = \frac{2\pi n R}{U_\infty} \qquad (2.2)$$

Where λ is the TSR (non-dimensional), R is the radius of the swept area (in meters), n is the rotational speed in revolutions per second, and V_∞ is the wind speed without rotor interruption (in meters per second).

The TSRs of the Savonius rotor and the multiple blade water-pumping windmills are generally low. In high-speed horizontal-axis rotors and Darrieus rotors, the outer tip actually turns much faster than the wind speed owing to the aerodynamic shape. Consequently, the TSR can be as high as 9. It can be said that high-solidity rotors have, in general, low TSRs and vice versa (Biswas et al., 2007).

Power Coefficient:

The power coefficient of a wind energy converter is given by

$$C_p = \frac{\text{Power output from wind machine}}{\text{Power contained in the wind}} = \frac{P_{out}}{P_w} \tag{2.3}$$

The power coefficient differs from the efficiency in the sense that the latter includes the losses in mechanical transmission, electrical generation, etc., whereas the former is just the efficiency of conversion of wind energy into mechanical energy of the shaft. In high-speed horizontal-axis machines, the theoretical maximum power coefficients are given by the Betz limit.

Wind Turbine Ratings and Specifications:

Since a wind turbine can produce varying amounts of electrical power depending on the wind speed, a standard procedure must be developed to specify the rating of a machine. One index used to compare various wind turbine designs is the specific rated capacity (SRC), defined as

$$SRC = \frac{\text{Power rating of the generator}}{\text{rotor swept area}} \tag{2.4}$$

The SRC varies between 0.2 for small rotors to 0.6 for large ones (Bhadra et al. 2005).

Choice of the Number of Blades:

Efficiency of power extraction depends on the proper choice of the number of blades. There will be less power extraction if the blades are so close to each other or rotate so fast that every blade moves into a turbulent air caused by the preceding blade. It will also be less than the optimum if the blades are so far apart or move so slowly that much of the air stream passes through the wind turbine without interacting the blade. Thus, the number of blades should depend on TSR. Let t_a be the time taken by one blade to move into the position occupied by the previous blade. For an n-bladed rotor rotating at an angular velocity ω,

$$t_a = \frac{2\pi}{n\omega} \tag{2.5}$$

Let t_b be the time taken by the disturbed wind, caused by the interference of the blade to move away and normal air to be re-established. It depends on the wind speed v and the length of the strongly perturbed wind stream, sayd, This length depends on the shape and size of blades:

$$t_b = \frac{d}{V} \tag{2.6}$$

For maximum power extraction t_a and t_b should both be approximately equal, so

$$\frac{w}{V} = \frac{2\pi}{nd} \tag{2.7}$$

For modem electricity-generating turbines, the empirical measurement of d and the requirement of a high TSR lead to a small number of blades, generally only two or three.

Though both 2- blades and 3- blade design is equally popular, the choice is dependent on some factors. The less nacelle weight and simplicity in erection are positive points by 2- blade turbine. In three-blade turbines 33% more weight and cost is involved, but the power coefficient improves by 5-10%. The 3- blade systems have a smooth power output, less blade fatigue and less chances of failure.

Capacity Factor:

The term Capacity factor refers to the capability of a wind turbine to produce energy in a year. It is defined as the ratio of the actual energy output of the energy that would be produced if it is operated at rated power throughout the year.

$$\text{Capacity factor} = \frac{\text{annual energy output}}{\text{rated power x time in a year}} \tag{2.8}$$

2.4 Power Speed Characteristics

The wind turbine power curves shown in figure illustrate how the mechanical power that can be extracted from the wind depends on the rotor speed. For each wind speed there is an optimum turbine speed at which the extracted wind power at the shaft reaches its maximum. Such a family of Wind turbine power curves can be represented by a single dimensionless characteristic curve, namely the C_p - λ curve, as in the figure, where the power coefficient is plotted against the TSR For a given turbine, the power coefficient depends not only on the TSR but also on the blade pitch angle. The figure shows the typical variation of the power coefficient with respect to the TSR λ with the blade pitch control. The mechanical power transmitted to the shaft is

$$P_m = 0.5\, \rho C_p U_\infty^3 A \qquad (2.9)$$

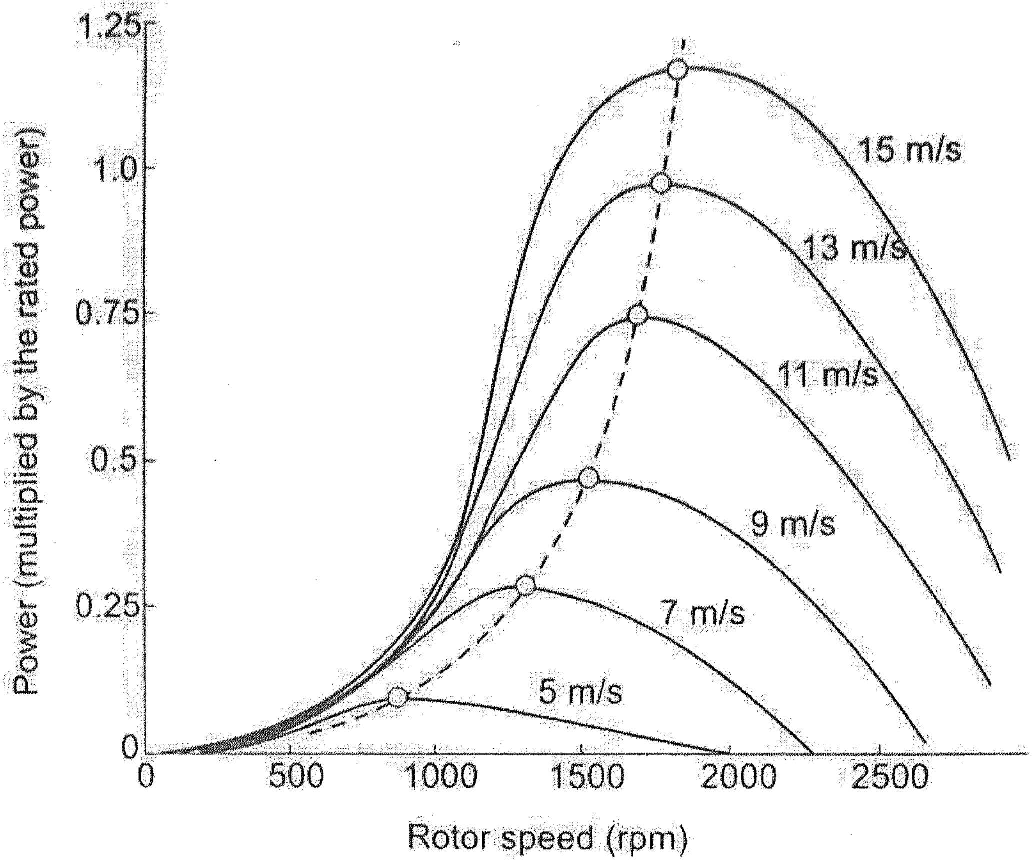

Figure 2.6: Power Speed Characteristics of Wind Turbine

Where C_p is the function of TSR λ and the pitch angle *a*.

For a wind turbine with radius R, it can be expressed

$$P_m = \frac{1}{2}\rho A C_p U_\infty^3 \quad , \quad A = \pi R^2 \qquad (2.10)$$

For a given wind speed, the power extracted from the wind is maximized if C_p is maximized. The optimum value of C_p, say $C_{p,opt}$, always occurs at a definite value of λ, say . This means that for varying wind speed, the rotor speed should be adjusted proportionally to adhere always to this value of $\lambda = \lambda_{p,opt}$, for the maximum power output from the turbine. Using the relation

$$\lambda = \frac{wR}{U_\infty} \qquad (2.11)$$

The maximum value of the shaft mechanical power for any wind speed can be expressed as

$$P_{max} = \frac{1}{2}\rho C_{p,pot}\pi\left(\frac{R^5}{\lambda^3_{opt}}\right)\omega^3 \qquad (2.12)$$

Thus the maximum mechanical power that can be extracted from the wind is proportional to the cube of the rotor speed, i.e., P_{max} is proportional to ω^3 (Qasim et al., 2011).

2.5 Torque Speed Characteristics

Studying the torque versus rotational speed characteristics of any prime mover is very important for proper matching the load and ensuring stable operation of the electrical generator. The typical torque speed characteristics of the two blade propeller- type wind turbine, the Darrieus rotor, and the Savonius rotor are shown in figure. The profiles of the Torque-speed curves shown in the figure follow from the power curves, since torque and power are related as follows

$$T_m = \frac{P_m}{w} \qquad (2.13)$$

From the equation, at optimum operating point $(C_{p,pot}, \lambda_{p,pot})$, the relation between the aerodynamic torque and rotational speed is,

$$T_m = \frac{1}{2}\rho C_{p,pot}\pi\left(\frac{R^5}{\lambda^3_{opt}}\right) w^3 \qquad (2.14)$$

It is seen that at the optimum operating point on the $C_p-\lambda$ curve, the torque is quadratically related to the rotational speed.

The torque speed characteristic curve shows that for the propeller turbine and the Darrieus rotor, for any wind speed, the torque reaches a maximum value at a specific rotational speed, and this maximum shaft torque varies approximately as the square of the rotational speed. In case of electricity production, the load torque depends on the electrical loading, and by properly choosing the load (or power electronics interface), the torque can be made to vary as the square of the rotational speed.

The choice of the constant of proportionality of the load is very important. At the optimal value, the Load curve follows the maximum shaft power. But a higher value, the load torque may exceed the turbine torque for most speeds.

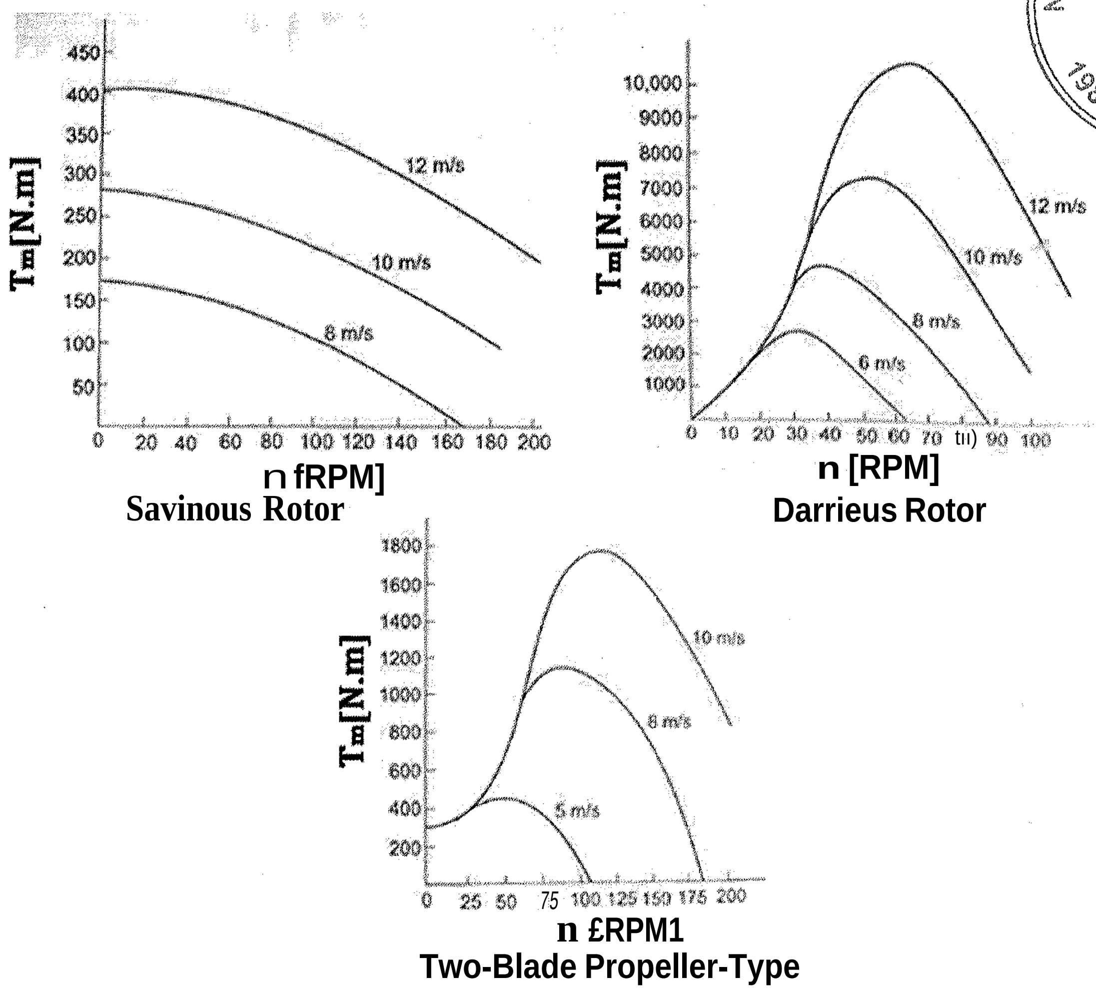

Figure2.7: The Torque Speed Characteristics of Various Wind Machines

Consequently, a machine would fail to speed up above a very low value. If the constant k is lower than the optimal value, the machine may over speed at the rated wind speed, activating the speed-limiting mechanism. Thus the proportionality constant of the load needs to be selected from a rather narrow range, about 10 -20 % of the optimum power curve. Note that the point of maximum torque is not the same as that of the maximum power.

As the power output is the product of torque and speed, it also has the maxim that varies as the cube of the rotational speed. The matching characteristics of the load can make the load curve pass through the maximum power points atall the wind speeds. For generators that feed power to the grid, the torque- speed characteristics are tuned using power controls.

In terms of the power coefficient C_p, the aerodynamic torque becomes

$$Tm = 0.5\, pCrVJA \tag{2.15}$$

WhereCT = C/lı. is called the torque coefficient (Bhadra et al., 2005).

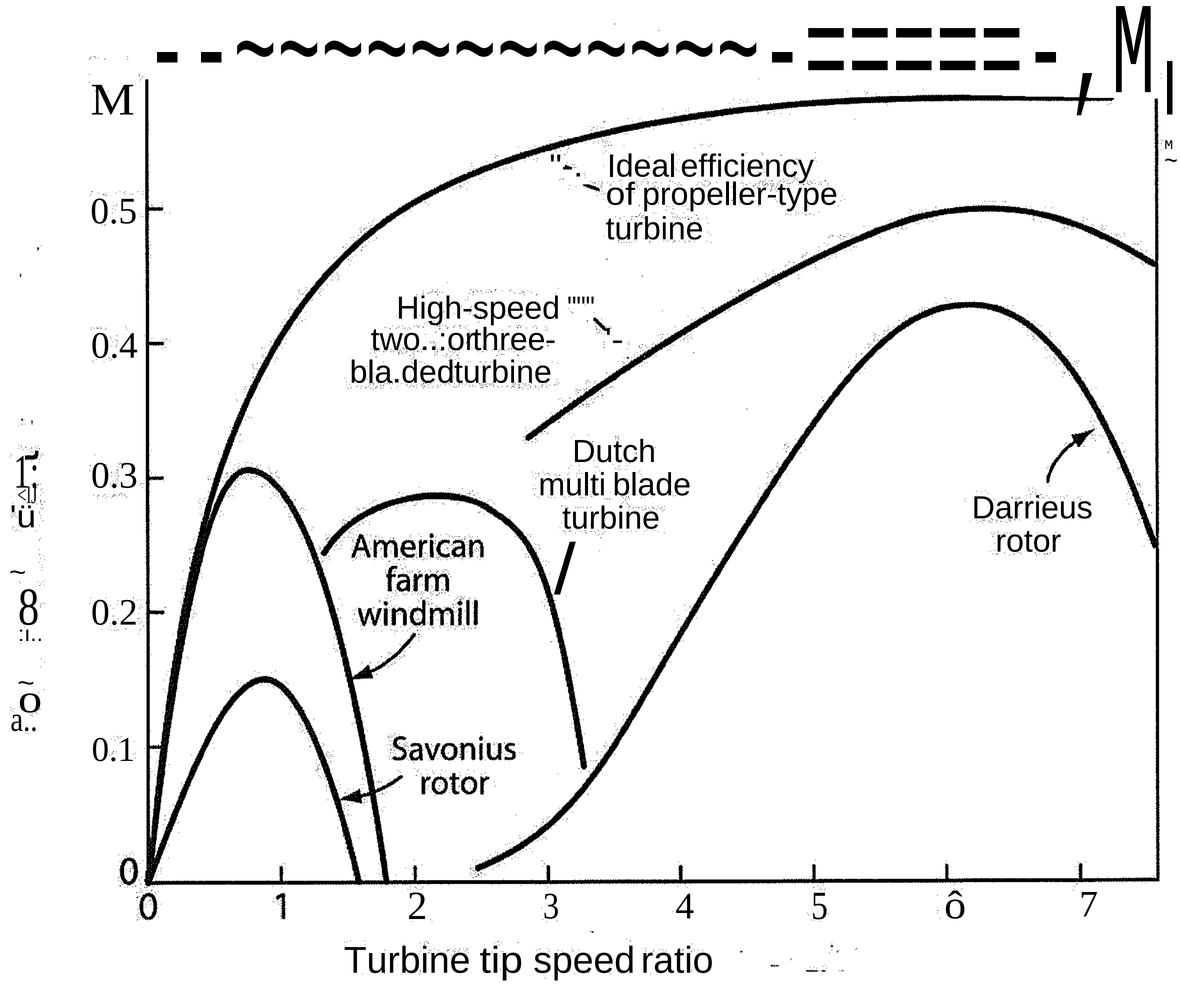

Figure2.8: Power Coefficient versus Turbine Tip Speed Ratio

CHAPTER3

SAVONIUS WIND TURBINE

3.1 Introduction

Researchers have been conducting lots of experiments on HAWT, because of its high efficiency. In some way, researchers have been trying their best to find the best from Darrieus rotor. Meanwhile, significant numbers of researchers have been working to improve the aerodynamic characteristics of Savonius turbine. These researches are numerical and theoretical prediction of flow around the wind turbines and from that it varies from research laboratories to full scale simulation. The extensive amount of work has been carried to find a sustainable solution of wind energy. Around the globe, researchers have been experimenting on HAWT and Darrieus rotor for large scale energy production and Savonius rotor for small scale usage. Based on the conclusion of those experiments, hybrid turbines are also a focus of the researchers. A brief discussion of Numerical analysis and experimental work on Savonius wind turbine will be discussed in this chapter.

3.2 Vertical Axis Wind Turbine

From history book, it was found that about 1300 A.Da Syrian cosmographer Al-Dimashqi drew a vertical axis windmill (Shepherd, 1990). It was a two storied wall structure with milestones at the top and a rotor on the bottom. It had latter with spooks reel with 6 to 12 upright ribs that covered with cloth. It was found that this type of windmill had been in operation in 1963 which used to produce an estimated 75 HP (at an efficiency of 50% at wind speed 30 mis). Each windmill milled one ton of grain per day (Wulff, 1967).

3.2.1. Savonius Wind Turbine

The Savonius wind turbine is one of simplest turbines. It can provide high starting torque and the manufacturing cost of the rotor blades can be very low. The standard Savonius rotor design or known as the conventional Savonius rotor was built of semi-cylindrical blade. Savonius wind turbine also can be categorized as 'small' type VAWT where its specialty is an omnidirection for accepting the drag force of wind and can produces the power from a few watts to 20 kW (Kadam and Patil, 2013).

Figure 3.1 shows the schematic drawing of drag forces exert on the blades of the conventional Savonius rotor. From the wind direction, the concave part caught the wind current and forces the blade to rotate about its central vertical shaft. It will experience more drag forces. However, the convex part will experience less drag forces as when the wind hits the blade and causes the air wind to be deflected a way around it. Hence, the differential drag causes the rotor to rotate and leads the Savonius turbine to spin (Ali, 2013).

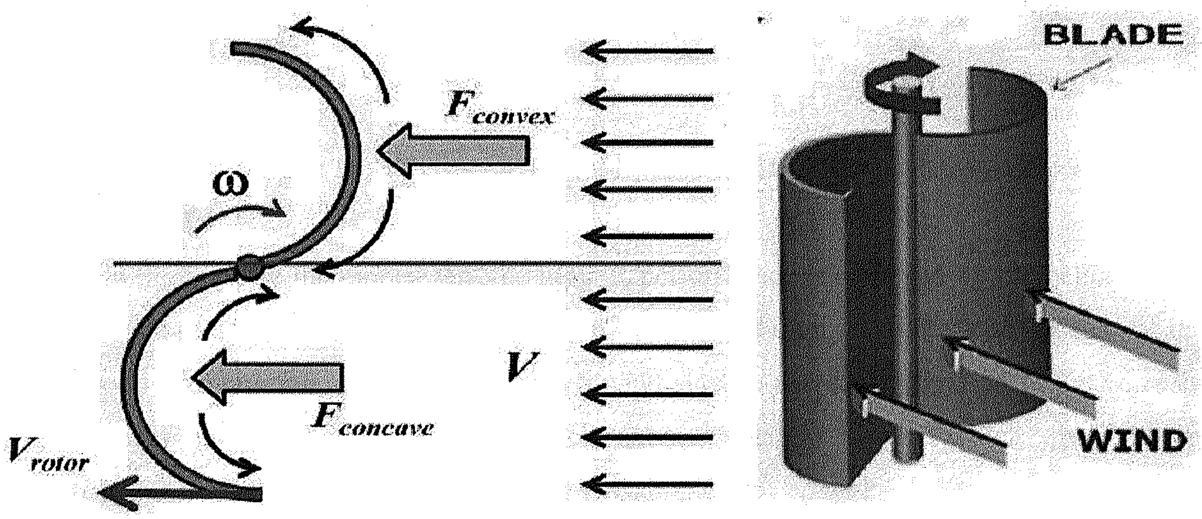

Figure 3.1: The Schematic Drawing of Drag Forces Exerted on Blades of Conventional Savonius Rotor

The design of the Savonius rotor gives the highest power coefficient compared to the Darrius rotor Norhazwani (2014). claimed that the power coefficient depends on the power generated and the swept area which is known as the cross-sectional area of the rotor. A smaller swept area of the turbine tends to generate a higher power coefficient. The power coefficient can be converted by the turbine into mechanical work where higher power coefficients will effects to a higher potential for the turbine to generate more power.

The conventional wind turbine is often used by researchers to complete their studies. However, some researchers had introduced a helical-shape blade Savonius wind rotor and study its performances Hu et al. (2009) stated that the performance in terms of the power coefficient (Cp) using helical-bladed Savonius was improved from Cp = 0.15 to Cp= 0.20. There are four types of helical rotor with different twisted angles shown in Figure 3.2. The twist angles are 90°, 180°, 270° and 360° respectively.

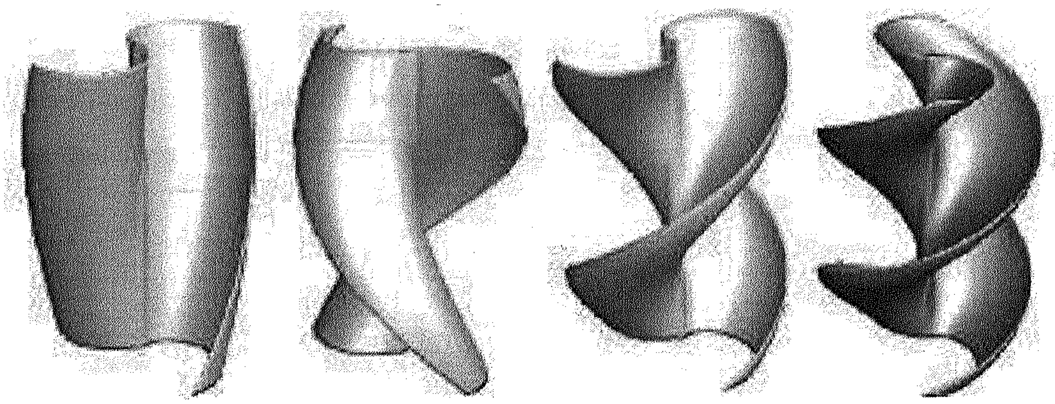

(a) 90° (b) 180° (c) 270° (d) 360°

Figure 3.2: The Four Types of Helical Rotor with Different Twisted Angle

From Ru's findings, he mentioned that the highest performance is achieved by the helical rotor with the angle of 180° and it can be observed in the graph shown in Figure 3.3. Because of its 180° helical configuration, the rotor has a downwind surface part that's exposed to the wind at any rotational angles. It also produces a continuous positive torque, which gives better performance than the helical rotor with another twist angle.

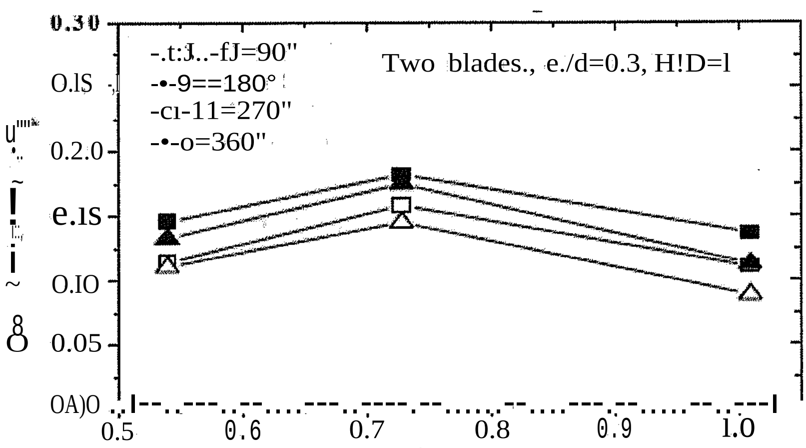

Figure 3.3: The Power Coefficient Performance Curve of Four Types of Helical Rotor

The research conducted by Can et al. (2010) had found that the torque performance of spiral rotor is better than the conventional rotor. Figure 2.4 below shows the variation of torque result with blade rotation angle. For conventional rotor, the maximum torque coefficient is 0.37 while the minimum is below than 0.05. It is also experiencing wavy variation. Whereas, the spiral rotor undergone some large fluctuations of torque coefficients where the maximum and the minimum torque coefficient is around 0.50 and 0.31 respectively.

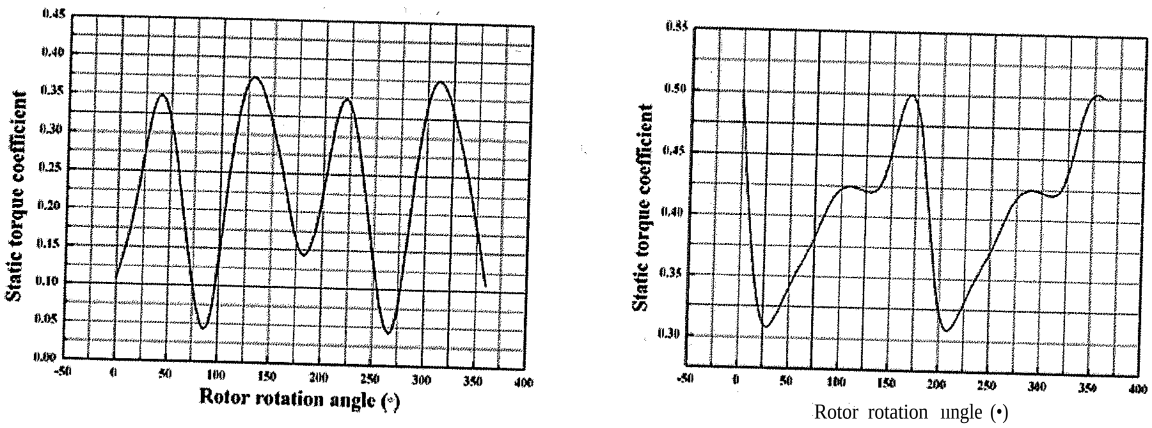

(a) Conventional Savonius rotor (b) Spiral rotor

Figure 3.4: Variation of Torque with Blade Rotation Angle

2.2.3 Number of Rotor Blades

The number of blades of the rotor should be minimized to two blades only. Ali (2013) found that the two-bladed Savonius wind turbine is more efficient and has a higher power coefficient compared to a three-bladed Savonius wind turbine under the same test condition. It is because as the number of blades increases, it will also increase the drag on the surfaces when the wind flows around them. This will cause the reverse torque to increase and causing the net torque working on the blades of Savonius wind turbine to decrease. Kadam and Patil (2013) also stated that, in order to increase the efficiency of the operation parameters, using two blade wind turbine is better compared to using either three blades or four blades rotors.

The evidence of using two blades was supported by Hu et al. (2009) where if the number of blades was increased from two to three, the power coefficient of the wind turbine rotor will decrease. Figure 3.5 shows the performance curve of both two blades and three blade rotor which explained that when TSR = 0.8, the power coefficient for two-bladed rotor is 0.165 while three-bladed rotor is 0.12. Meanwhile, Figure 3.6 shows the fluid field of two-bladed and three-bladed rotor. The two-bladed rotor has a bigger downwind pressure surface compared to the three-bladed rotor which has a bigger upwind pressure surface. To obtain a better rotor performance, the pressure on downwind surface should be bigger and upwind surface is smaller.

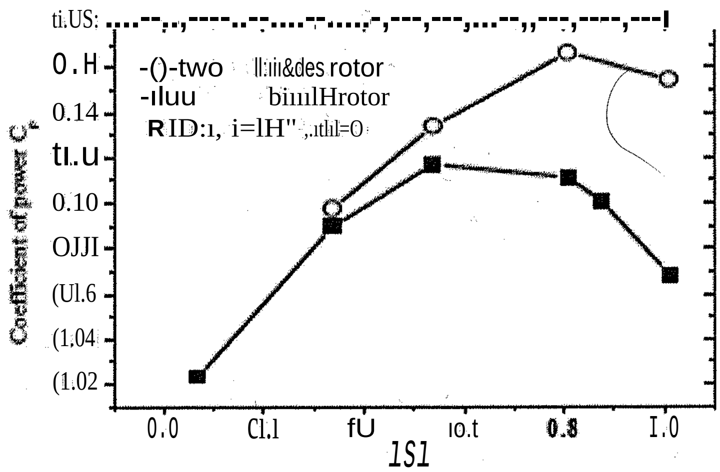

Figure 3.5: The Performance Curve of Two and Three Blade Rotor

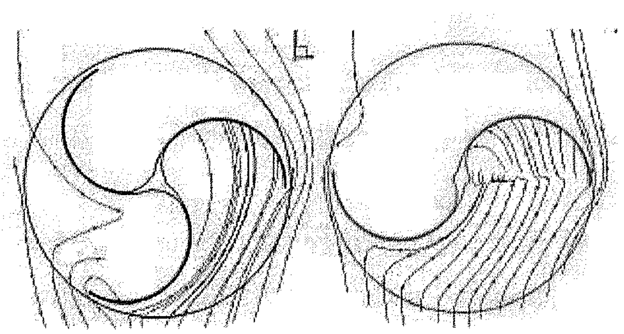

Figure 3.6: The Fluid Field of Two and Three Blades Rotor

3.3 Reviews on Savonius Rotor

The optimum output from the wind energy is the key objective of the investigation and different aerodynamic shapes of the blades are designed to verify the outcome. Numerous investigations had been carried out in the past to study the performance characteristics of Savonius rotor. These investigations included wind tunnel tests, field experiments and numerical studies. Blade configurations were studied in wind tunnels to evaluate the effect of aspect ratio, number of blades, overlap and gap between the blades, effect of adding end extensions, end plates and shielding.

The performance of two bladed Savonius turbine with five overlaps of 16.2%, 20%, 25%, 30% & 35% were investigated. Among them, 16.2% overlap condition showed maximum power extraction. The pressure drop across the rotor from upstream to downstream as well as, the maximum pressure difference across the returning bucket was displayed-in-the same condition which eventually indicated the better overall aerodynamic torque and power (Gupta et al., 2012). Three bladed Savonius rotor with different overlap ratio was taken care for another experiment. A ratio of 0.0, 0.12 and 0.26 had been used for different Reynolds number (Re). The model with no overlap ratio showed a better torque coefficient for lower Re, better power coefficient at higher Re and with the increase of the tip speed ratio (Morshed, 2010).

Biswas et al. (2007) conducted the experiment on three bladed Savonius turbine in front of sub-sonic wind tunnel with no overlap and for overlap conditions in the range 'of 16% to 35%. They found out that, at no overlap condition, maximum power factor is 36% without blockage correction at TSR of 0.50, and 28% with blockage correction at TSR of 0.46. With the increase of overlap ratio, the values of power-coefficient decreased for blockage effects. Power coefficients increased with the increase of the overlap ratio up to a certain limit and afterwards start decreasing even the overlap is increased. From this experiment, the maximum power coefficient was found 47% without blockage correction and 38% with blockage correction at 20% overlap.

Qasim et al. (2011) worked with impeller scoop-frame type with movable vanes wind turbine VAWT. The objective was to maximize the drag factor by closing the vanes on convex shape and open when air hit the concave part. Due to movement of vanes for and against of wind, a higher drag factor had worked on the impeller scoop-frame type with movable vanes, and had a higher efficiency than flat vanes.

Manzoor et al. (2008) experimented on the Savonius rotor to compare the performance of twisted blade. Initially they carried the experiment with two vertical, semi-circular curved blades and then with twisted blades with the angle ranging from 0° to 60°. From the analysis of wind flow over various configurations of the rotor blades, they have concluded that, the maximum efficiency of 33.85% had been found at 8=45° compared to 25.6% without twist. This twist increases the positive wetted /pırt in the side projected area which results an increase in the average projected area. At the same twist angle, both the RPM and torque were also obtained higher than without twist.

Saha et al. (2006) studied the performance of twisted blade. All the tests were carried out in a three-bladed system with a blade aspect ratio of 1.83. The study s~ôwed that, a potential of smooth running, higher efficiency and self-starting capability had beeh~ere for twisted blades compared to semicircular blades. Comparatively larger twist angle provides maximum power and better starting characteristics at lower wind velocity. The optimum performance is displayed at lower airspeeds of 6.5 *mis* and twist angle of a =15° in terms of starting acceleration and maximum no load speed.

Ghatage and Joshi (2012). have done a further experiment by changing twist of the blade as well as the number of blades. They have studied with both regular blade and twisted blade. The experiment concluded that two blades with twist enhance the efficiency of turbine. In their experiment the two-bladed 30° twisted bladed turbine gave the better power coefficient. It was concluded that the twisted blade attributes relatively higher drag on the turbine surface.

Ghosh, et al. (2009) has experimented Single- and three-stage modified Savonius rotors, which are extensively tested in front of an open jet wind tunnel. With the increase in the Reynolds number both the single- and three-stage rotors shows higher coefficient of power. The three-stage rotor showed positive and a uniform coefficient of static torque. Here the number of blades also had some effect. The coefficient of static torque differed with the change of blade number in a three-stage rotor.

Hayashi et al. (2005) experimented a wind tunnel test to improve the starting characteristics of Savonius rotor with and without guided vanes. They have concluded that, the three staged rotor had a better torque coefficient than the single stage rotor. The guide vanes further increased the torque coefficient.

Kumbemuss et al. (2012) studied two-staged Savonius-type turbines with different number of blades, the shape of the blades, the overlap ratio and the phase shift angle. The wind turbines were tested under four different wind speeds of 4m/s, 6m/s, 8m/s and 1Om/s. There were three turbines with the overlap ratios of 0, 0.16 and 0.32. Before testing those in an open wind tunnel, the wind turbines were adjusted to the phase shift angles (PSA) of 0, 15, 30, 45 and 60 degrees under different air velocities. The overlap ratio of 0.16 produced the better performance among the three, followed by the 0.32 overlap ratio. At lower air velocities the larger phase shift angles and at higher air velocities smaller phase shift angles will produce better performance of the turbines.

Saha et al. (2008(conducted a wind tunnel test to assess the aerodynamic performance of Savonius rotor systems with different stages. Both semicircular and twisted blades had been used in each case. Experiments were carried out to optimize the different parameters like number of stages, number of blades (two and three) and geometry of the blade (semicircular and twisted). It was concluded from this experiment that, two-stage rotor showed a better performance characteristics when compared the three-stage rotor. As the number of stages was increased, the inertia of the rotor was found to increase thereby reducing its performance. This was independent on the blade geometry. Two-bladed system gave optimum performance and in a two bladed system, the performance of twisted-bladed rotor was superior to the semicircular-bladed rotor.

Diaz et al. (1991) analyzed to find the drag and lift coefficients of a Savonius wind turbine to find the aerodynamic performance. They found that at a tip-speed ratio of $\lambda = 1$ the rotor operated with maximum efficiency, in terms of power coefficient. For either increase or decrease of tip-speed ratio the drag coefficient decreases sharply. They also suggested that, around tip-speed ratio $\lambda = 1$, Savonius rotor operates most efficiently, where there is almost no effect of change oflift force due to the coefficient remains constant at 0.5.

Rahman et al. (2009) experimented on the Drag and Torque characteristics of three bladed Savonius Wind Turbine. The turbines with no overlap has better drag and torque characteristics. They also performed Aerodynamic performance analysis on three bladed Savonius wind turbine and concluded that higher Reynolds number showed better aerodynamic behavior for no overlapping blades.

Carrigan et al. (2012) had the objective to introduce and demonstrate a fully automated process for optimizing the airfoil cross-section of a VAWT. The objective was to maximize the torque while enforcing typical wind turbine design constraints such as a tip speed ratio, solidity, and blade profile. This work successfully demonstrated a fully automated process for optimizing the airfoil cross-section of a VAWT. As this experiment was not an extensive study, so they had suggested further research and development.

Choudhury and Saraf (2014}made numerical analysisusing (computational fluid dynamic (CFD) software ANSYSFLUBNT) on a two-Bladed Savonius Rotor. They studied drag and torque coefficient curves at different rotor blade angles at each 10° interval. These curves show that the drag and torque EemcientS'Teached its maximum at 0' and 30' rotor blade angles respectively.

Ali (2013) carried out an experimental study using subsonic wind tunnel under low wind speed. Also, he compared and investigated the performance of two and three blades of Savonius wind turbine rotor. He concluded that increasing the number of blades will increase the drag surfaces against the wind air flow and causes it to increase the reverse torque and leads to a decrease in the net torque working on the blades of a Savonius wind turbine.

Konrad et al. (2013) investigated numerically, the running performance of three different types of Savonius wind turbine rotor namely classical, Bach-type and Elliptical designs, using ANSYS CFX. The running performance of the Savonius rotor, such as the torque coefficient, is obtained for various tip speed ratios; It is found that the Bach-type has a maximum torque coefficient than other types. Also, in terms of power coefficient the Bach type rotor is superior to other tested geometries and at the same time, the Elliptical Savonius turbine exhibits better power characteristics than the classic one.

Kawamura et al. (2001) investigated the running performance of the rotor, using a domain decomposition method. Two computational domains were used and connected to each other. One domain contains the rotating rotor and the other contains the fixed walls; both domains have common overlapping regions. The running performance of the Savonius rotor, such as the torque coefficient, is obtained for various tip speed ratios. The effects of the walls on the running performance were also investigated. It was found that the power coefficient has been raised significantly.

Sargolzaei (2007) predicted the power factor and torque of wind turbines using artificial neural networks (ANNs) based on experimental data that were collected over seven prototype vertical Savonius rotors. The simulation and experimental results were compared and it showed that the simulation has the capability of providing reasonable predictions for the maximum power of rotors and maximizing the efficiency of Savonius wind turbines. Also, according to his results, increasing Reynolds number leads to an increase in power ratio and torque.

Gad et al. (2014) discussed numerically a modified Savonius wind rotor focusing on the averaged torque and power coefficients over a complete cycle of operation by using the commercial software Fluent 6.3.26 with four different turbulence models. The results showed that the modification of the blades of the rotor causes an increase of the performance of the rotor. Kamoji et al. (2008) s~di~d experimentally the torque of a conventional Savonius rotor for variable overlaps ratio, blade edge condition and change in Reynolds number. The results showed the coefficient of static torque decreases as the overlap ratio is increased. Also, it showed that the power coefficient increases with an increase in the Reynolds number, whereas the coefficient of static torque is independent of the Reynolds number. And the coefficient of power, torque coefficient and coefficient static torque are independent of blockage ratios at a given Reynolds number.

Saha et al. (2008) discussed the aerodynamic performance of single-, two- and three-stage Savonius rotor systems based on experiments that were carried out to optimize the different parameters like number of stages, number of blades and geometry of the blade. In addition, all the experiments were conducted at different wind speed. The results showed that a twisted geometry blade profile had better performance as compared to the semicircular blade geometry, the two-stage Savonius rotor had a better power coefficient as compared to the single- and three-stage rotors.

Fox el at. (2002) experimentally studied the effect of end plates with various shapes and size on the aerodynamic performance of helical Savonius wind turbine with twist angle and two semi-circular buckets. The results showed the power coefficient increased linearly in proportion to the area of the end plate.

Bhaumik et al. (2010) measured experimentally the power coefficient of a two-bladed helical Savonius wind rotor at the exit of a centrifugal blower for five different overlap ratios.

Kamoji et al. (2009) evaluated the power and static torque coefficient of a helical Savonius rotor were evaluated in an open jet wind tunnel test under various design and operating conditions.

3.4 Savonius Wind Turbine Theory

As the simplest turbine, Savonius wind turbine works due to the difference of forces exerted on each blade. The concave part to the wind direction catches the wind and forces the blade to rotate around its central vertical shaft. On the other hand, the convex part hits the air wind and causes the blade to be deflected sideways around the shaft. The blade curvature has less drag force when moving against the wind of F_{convex} than the blades moving with the wind of $F_{concave}$ as seen in

Figure 3.7 (USA Alternative Energy NOW, 2010). Hence, concave blades with more drag force than the other half cylinder will force the rotor to rotate.

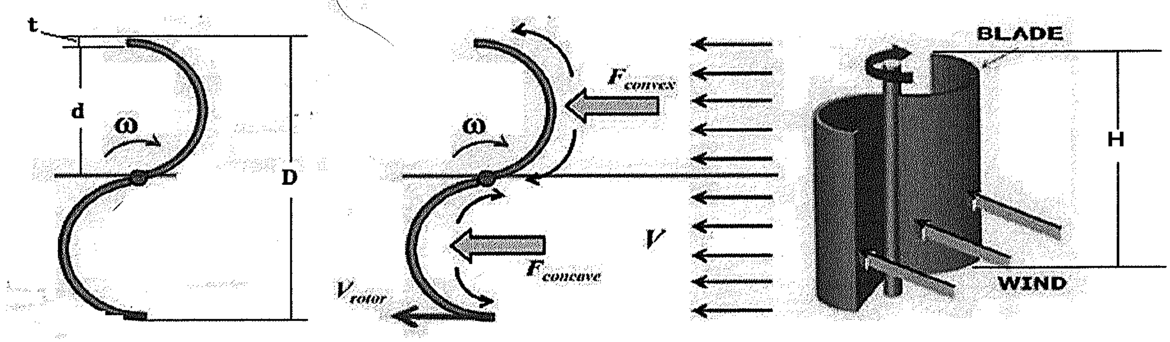

Figure 3.7: Two Blades Savonius Wind Turbine with the Drag Forces

The performance of Savonius wind turbine can be expressed in the form of torque coefficient (Ct) and the coefficient of power (Çp) in comparison with the tip speed ratio or TSR is a parameter related with rated wind speed and rotor diameter. As the ratio between the speed of tip blade and wind speed through the blade, TSR can be determined as (GWEC, 2006).

$$TSR = \lambda = \frac{V_r}{V_w} = \frac{\omega R}{V_w} \tag{3.1}$$

Where Yr is the tip speed of the peripheral velocity of rotor (m/s); ro is the angular velocity of the rotor (1/s); dis the diameter of halves cylinder of rotor (m), and Vw is the wind speed (mis).

The coefficient of torque is defined as the ratio between the actual torque develop by the rotor (T) and the theoretical torque available in the wind (Tw) as,

$$Ct = \frac{T}{T_w} = \frac{4T}{\rho A_s d V_w^2} \tag{3.2}$$

where p is the density of air (=1.225 kg/rrr^3); Tis the torque (N.m) and As is the swept area of blades = the rotor height x the rotor diameter (m^2).

The coefficient of power of a wind turbine (Cp) is the ratio between the maximum power obtained from the wind (Pt) and the total power available from the wind (Pa) as,

$$C_p = \frac{P_t}{P_a} = \frac{P_t}{\frac{1}{2}\rho A V_w^3} \tag{3.3}$$

Where the maximum poJ~~f a wind turbine is determined as (Frederikus et al., 2015).

$$P_t = T\omega \qquad [Watt] \tag{3.4}$$

CHAPTER4

AERODYNAMIC FORCES

When the wind blows, it exerts some forces on all the objects that are touched by the wind. The size and direction of these forces are evident in some cases and you can easily observe the effects. This chapter describes the two main forces of wind on a stationary object. These are lift and drag. Lift and drag are the two components of the total force from wind. Also, there are two coefficients associated with these forces components.

4.1 Force from Wind

When an object is in the path of the wind it is subject to two forces from wind. This is true for an object in the path of any fluid that moves, like water flowing in a pipe or a river. For the sake concentration of the wind only. The simplest case to start with is a plate with rectangular shape as shown in Figure 4.1 shows a plate that lies in the path of the wind at an angle with the wind direction. The direction of wind in Figure 4.1 is from left to right. As shown at the top of the figure, when the wind blows it pushes the plate. This is due to force component parallel to the wind direction. On the other hand, as wind passes through, depending on the angle of the plate with the direction of wind, it causes the pressure on the two sides of the plate to be different. The result of this pressure difference is a force that pushes is from the plate to one side (in Figure 4.1 it pushes the plate upward). This push is from the side with higher pressure to the side with lower pressure. This lower or higher pressure is due to the speed of the wind that is disturbed because of the plate. In addition to the above mentioned two force components, one more effect of the wind is to cause a rotation of the plate. This rotation is due to a torque.

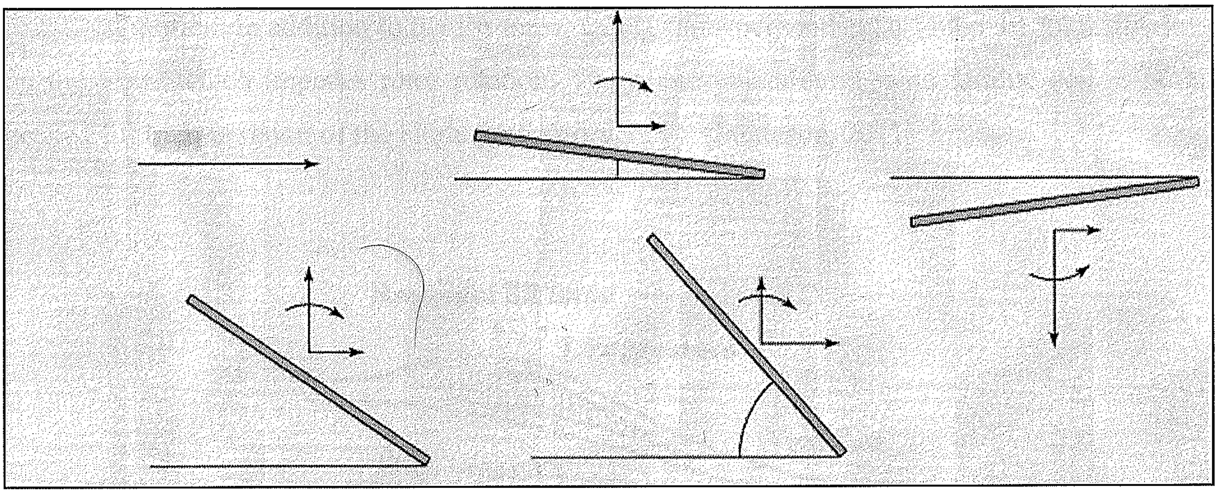

Figure 4.1: Three Cases Showing in which the Angles of the Plate with Different Wind Direction

4.2 Aerodynamic Forces

Aerodynamic force is exerted on a body by the air (or some other gas) in which the body is immersed, and is due to the relative motion between the body and the gas (Kothari et al., 2008) Forces acting on airfoils in motion relative to the air (or other gaseous fluids).

The force from the wind on a plate, just as studied in the previous section, is called aerodynamic forces. We referred to the two aerodynamic force component as lift and drag; any force can be broken into two components. Here the lift force and drag force are the two components of the aerodynamic force on the plate under consideration. There two components are perpendicular to each other; that is, they make an angle of 90° with each other as shown in Figure 4.1

4.3 Aerodynamic Operation of Wind Turbines

Aerodynamics deals with the movement of solid bodies through the air. In wind turbines, aerodynamicsprovides a method to explain the relative motion between airfoil and air. Airfoil is the cross-section of wind turbine blade. When the wind passes over the surface of rotor blade, it automatically passes over the longer or upper side of the blade, creating a low pressure area above the airfoil as shown in Figure 4.2 a.

The pressure difference between the top and the bottom surfaces results in a force called aerodynamic lift that causes the airfoil to rise. As the blades can only move in a plane with the hub as their center, the lift force causes rotation about the hub (Figure 4.2 b). The turbine, thus extracts energy from the wind stream by converting the wind's linear kinetic energy into rotational motion. In additionto the lift force, a drag force perpendicular to the lift force also acts on the blade which impedes rotor rotation. The prime objective in wind turbine design is the desired lift to drag ration of the blade (airfoil structure) (Jamieson, 2011).

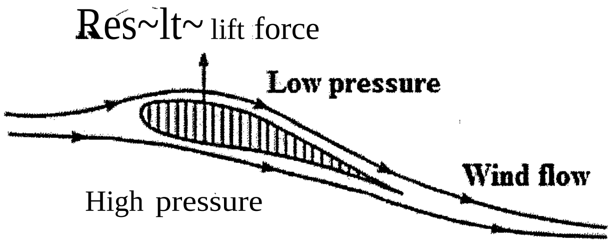

(a) Aerodynamic Lift Force on Blade Cross-Section of Wind Turbine

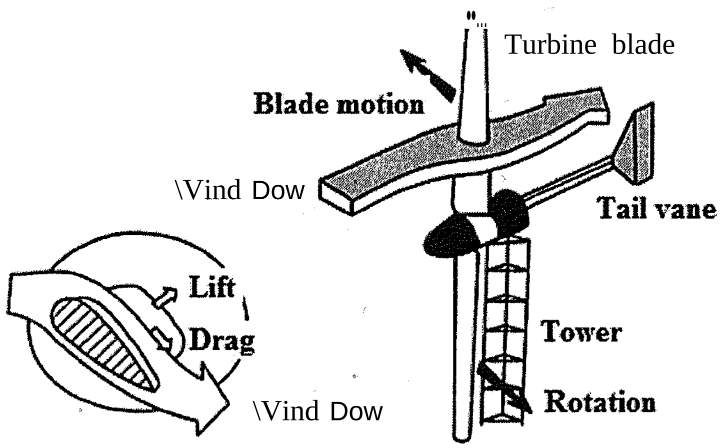

(b) the Basic Operation Principle of Wind Turbine Aerodynamic Lift

Figure 4.2: Aerodynamic operation of wind turbines

4.3.1 Lift and Drag Force on Airfoil

A fluid flowing past the surface of a body exerts a surface force on it. Lift is defined to be the component of this force that is perpendicular to the oncoming flow direction. It contrasts with the drag force, which is defined to be the component of the surface force parallel to the flow direction.

The equations for calculating lift and drag are very similar. The lift that an airfoil generates depends on the density of the air, the velocity of the airflow, the viscosity and compressibility of the air, the surface area of the airfoil, the shape of the airfoil, and the angle of the airfoil's angle of attack. However, depending on the airfoil shape, the angle of attack, air viscosity and compressibility are very complex. Thus, they are characterized by a single variable in the lift equation, called the lift coefficient. Due to the complexities of the lift coefficient, it is generally found via experimentation in a wind tunnel where the remaining variables can be controlled. Therefore, the lift equation is given by:

$$F_L = \frac{1}{2} V_w^2 \rho C_L A \tag{4.1}$$

Where F_L is the lifting force, ρ is the density of air, V_w is the relative velocity of the airflow A is the area of the airfoil as viewed from an overhead perspective, and C_L is the lift Coefficient.

As with lift, the drag of an airfoil depends on the density of the air, the velocity of the airflow, the viscosity and compressibility of the air, the surface area of the airfoil, the shape of the airfoil, and the angle of attack.

The complexities associated with drag and the airfoil shape, angle of attack, the air's viscosity, and air's compressibility are simplified in the drag equation by use of the drag coefficient. The drag coefficient is generally found through testing in a wind tunnel, where the drag can be measured, and the drag coefficient is calculated by rearranging the drag equation

$$F_D = \frac{1}{2} V_w^2 \rho C_D A \tag{4.2}$$

In the drag equation, F_D is the drag force, ρ is the density of the air, V_w is the velocity of the air, A is a reference area, and C_D is the drag Coefficient (Patrol, 2015).

The drag force is the net exerted by a fluid on a body in the direction of flow due to the combined effects of wall shear and pressure forces.

The part of drag that is due directly to wall shear stress is called the skin friction drag or just friction drag since it is caused by frictional effects, and the part that is due directly to pressure is called the pressure drag or called the form drag because of its strong dependence on the form or shape of the body.

'4.3.2 Types of Drag

As already mentioned, the drag is the resistive force encountered by the body when it is moving through a fluid or when the fluid flows past a solid body. In both cases, in order to maintain steady motion, a force is the direction of relative motion has to be exerted. Thus, when the submarine moves through water o1an-a~-plane flies through the atmosphere, the vehicle has to exert a forward force sufficient enough to balance the drag force. Drag force may be related to the effect of boundary layer, flow separation and wake. The existence of viscosity for the fluid is mainly responsible for causing drag on bodies.

The total drag may be separated into a number of items each contributing to the total. As first step, it is divided into friction drag and pressure drag.

4.3.2.1 Friction Drag

Due to the viscous nature of fluid, the fluid motion tends to be rotational which gives rise to velocity gradient in the thin boundary layer region. In the laminar boundary, since the adjacent fluid layers move with different velocities, tangential shear stress is set up. In the turbulent layer, since there is velocity fluctuation, additional shear stress is set up. These shear stresses leads to the shear drag or friction drag, friction drag does not exist in a flow assumed to be inviscid.

4.3.2.2 Pressure Drag

The drag force arising from the resolved components of the pressure on the boundary is the pressure drag. The pressure drag may itself be considered as sum of the several distinct items.

i. Form Drag

Form drag is mainly due to the wake formed behind anybody having relative motion with the fluid. When the surface of the body is not parallel to the flowing stream, the flow pattern get considerably modified due to boundary layer growth and separations form the surface of the body. The separated flow gives rise to a low pressure region called wake on the rear side of the body. The pressure difference between the two sides of the body gives rise to pressure drag, which is referred to as form drag. Figure 4.3 a, b and c gives an indication of the comparative width of the wake behind a few bodies. Its magnitude depends on the size of the wake which depends on the position of separation points.

ii. Wave Drag

The wave drag is due the waves formed in the flow, in compressible flow, it is due to the formation of compression shock wave.

iii. Induced drag

The induced drag is due to the trailing vortex formed due to the flow past the body, it depends on the lift force.

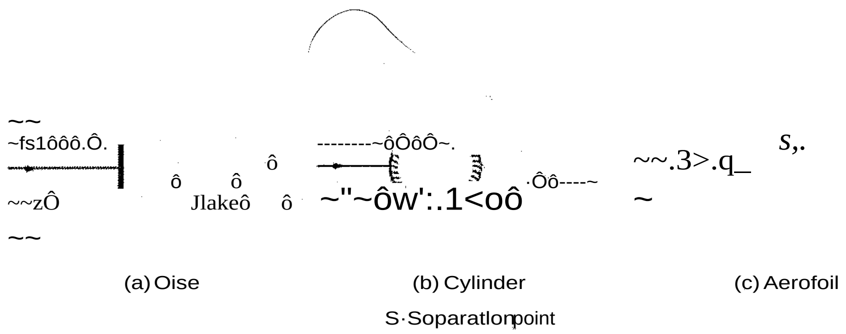

Figure 4.3: Wake behind Stationary Bodies

If the wave drag and induced drag are neglected, then the total drag is essentially the skin friction drag and the form drag (Balachandran, 2011).

4.3.3 Drag Coefficient

In fluid dynamic, the drag coefficient (commonly denoted as: Coor Cw) is a dimensionless that is used to quantify the drag or resistance of an object in a fluid environment such as air or water. It is used in the drag equation, where a lower drag coefficient indicates the object will have less aerodynamic drag. The drag coefficient is always associated with a particular surface area. The drag coefficient of any object comprises the effects of the two basic contributors to fluid drag: skin friction and form drag. The drag coefficient of a lifting airfoil also includes the effects of lift-induced drag. The drag coefficient of a complete structure such as an aircraft also includes the effects of interference drag. The drag coefficient Cois defined as:

$$Co = \frac{2Fv}{pVJ,A} \qquad (4.3)$$

Where,

Fv is the drag force, which is by definition the force component in the direction of the flow velocity,

p is the mass density of the fluid,

Vwis the speed of the object relative to the fluid, and

A is the reference area'(Fox et al., 2002).

Drag on airfoils arises from viscous and pressure forces. Viscous drag or Skin friction changes with Reynolds number and arises from the interaction between the fluid and the skin of the body but only slightly with angle of attack. These relat.i~hips and some commonly used terminology are illustrated in Figure 4.4.

A useful approximation to drag polar for complete aircraft may be obtained by adding the induced drag or vortex drag, or sometimes drag due to lift, is a drag force that occurs whenever a moving object redirects the airflow coming at it to the drag at zero lift. The drag at any lift coefficient is obtained from

$$C_O = C_{O,0} + C_{O,i} = C_{O,0} + \frac{C_t}{rrar} \quad , \quad ar = \frac{b^2}{p} \tag{4.4}$$

Where,

$C_{O,0}$: drag coefficient at zero lift

$C_{O,i}$: induced drag coefficient

ar: Aspect ratio

b: wingspan or is the distance from one wingtip to the other wingtip of the airplane

Ap: Planform area

c: chord length (Graebel, 2001).

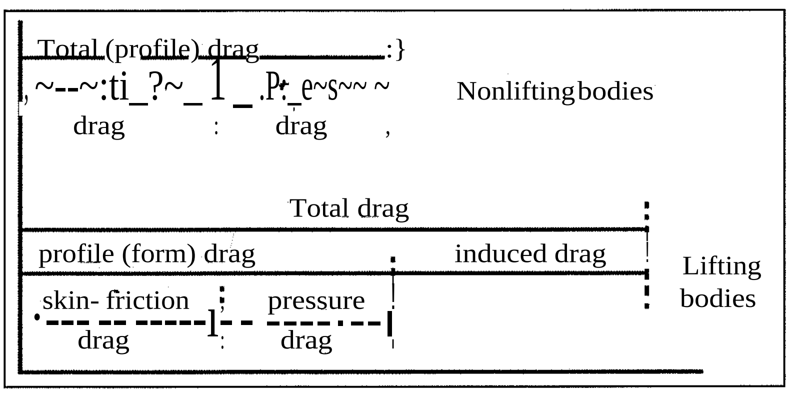

Figure 4.4: Drag Breakdowns on Non-Lifting and Lifting Bodies

The drag coefficient for all objects with sharp edge is essentially independent of Reynolds number (for $Re \geq 10000$) because the separation points and therefore the size of the wake are fixed by the geometry of the object. Drag coefficients for selected objects are given in Table 4.1

4.3.4 Friction Coefficient

The friction coefficient for laminar flow over a flat plate can be determined theoretically by solving the conservation of mass and momentum equations numerically. For turbulent flow, however, it must be determined experimentally and expressed by empirical correlation. The local friction coefficient varies along the surface of the flat plate as a result of the changes in the velocity boundary layer in flow direction. We are usually interested in drag force on the entire surface, which can be determined using average friction coefficient. But sometimes we are also interested in the drag force at a certain location, and in such cases, we need to know the local value of the friction coefficient. With this in mind, we present correlations for both local (identified with the subscript x) and average friction coefficients over a flat plate for laminar, turbulent, and combined laminar and turbulent flow conditions. Once the local values are available, the average friction coefficient for the entire plate can be determined by integration from

$$C_f = \frac{1}{L}\int_0^L C_{f,x}\,dx \tag{4.5}$$

Based on the analysis, the boundary layer thickness and the local friction coefficient at location x for laminar flow over a flat plate were determined by

$$\text{Laminar:} \quad \delta = \frac{4.91x}{Re_x^{1/2}} \quad \text{and} \quad C_{f,x} = \frac{0.664}{Re_x^{1/2}} \qquad Re_x < 5 \times 10^5 \tag{4.6}$$

$$\text{Turbulent:} \quad \delta = \frac{0.38x}{Re_x^{1/5}} \quad \text{and} \quad C_{f,x} = \frac{0.059}{Re_x^{1/5}} \qquad 5 \times 10^5 \leq Re_x \leq 10^7 \tag{4.7}$$

where x is the distance from the leading edge of the plate and $Re_x = Vx/\nu$ is the Reynolds number at location x. Note that $C_{f,x}$ is proportional to $1/Re_x^{1/2}$ and thus to $x^{-1/2}$ for laminar flow and it is proportional to $x^{-1/5}$ for turbulent flow. In either case, $C_{f,x}$ is infinite at the leading edge ($x = 0$), and therefore Eqs. 4.6 and 4.7 are not valid close to the leading edge. The local friction coefficients are higher in turbulent flow than they are in laminar flow because of the intense mixing that occurs in the turbulent boundary layer. Note that $C_{f,x}$ reaches its highest values when the flow becomes fully turbulent, and then decreases by a factor of $x^{-1/5}$ in the flow direction. The average friction coefficient over the entire plate is determined by

$$\text{Laminar,}\quad C_f = \frac{1.33}{\sqrt{Re_L}} \qquad Re < 5 \times 10^5,$$

$$\text{turbulent,}\quad C_f = \frac{0.074}{Re_L^{1/5}} \qquad 5 \times 10^5 < Re < 10^7 \qquad (4.8)$$

Table 4.1: Drag Coefficient Data fo\~elected Objects (Re~l 04).

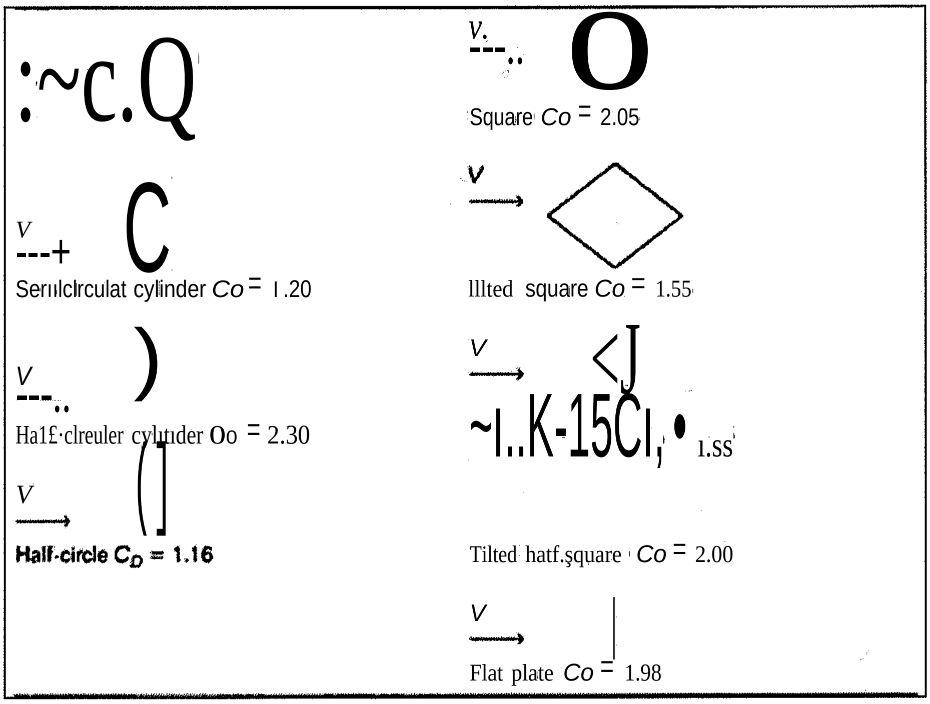

4.4 Estimate the Torque and Mechanical Power Output

As discussed earlier, the Savonius type rotor is a drag-based wind turbine because it's the drag component of the aerodynamic force that powers the Savonius turbine to rotate. There are two types of Savoniuswind turbine rotor as shown in Figure 4.5.Figure 4.5 shows a schematic models of Savonius wind rotor. The model has a different Savinous rotor type. We can estimate the torque, and mechanical power output of a Savonius rotor using a simplified model, Figure 4.6. This simplified model, however neglects the effect of rotor on the wind flow characteristics.

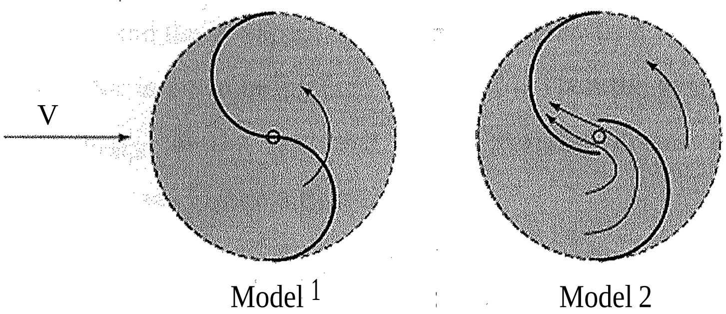

Figure 4.5: Models bvonius Rotor

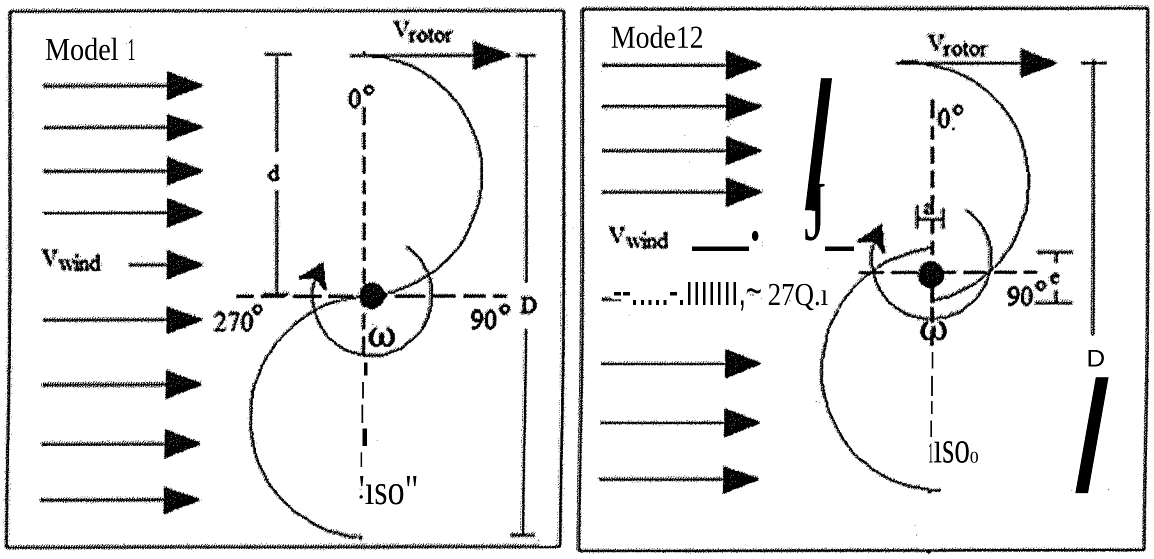

Figure4.6: Schematic Diagram of a Different Two -Bladed Savonius Rotor

Let's assume that the rotor has mean radius R and it is rotating with an angular speed ω. The circumferential velocity of the rotor or rotor velocity, V_r, at the mean radius is equal to:

$$V_r = wR \tag{4.9}$$

during the rotation, the wind velocity is broken into two components: X, and Y as shown in Figure 4.7. Vertical flows were not considered in this research, and could be a topic for future exploration. Assuming that the axis of the C-section vertical axis wind turbine rotor is the upward-pointing Y-axis, the flow experienced in the X-direction is the sum of the free-stream flow in the X-direction, and the X-aspect of rotational velocity (see Figure 4.8).

Let assume that the rotor is not rotating (see Figure 4.6). Then the average relative velocities of the wind $V_{rel,1}$ and $V_{rel,2}$ at the first and second rotating drums are given by following expressions, respectively (see Figure 4.8).

$$v_{rel,1} = v_w - v_r \tag{4.10}$$

$$V_{rel,2} = V_w + V_r \tag{4.11}$$

The resulting drags forces $F_{v,1}$ and $F_{v,2}$ on the rotating drums are given as:

$$F_{v,1} = \frac{1}{2}\rho C_{v,1} V_{rel,1}^2 A = \frac{1}{2}\rho C_{v,1} A (V_w - V_r)^2 = \frac{1}{2}\rho C_{v,1} A V_w^2 \left(1 - \frac{V_r}{V_w}\right)^2 \tag{4.12}$$

$$F_{v,1} = \frac{1}{2}\rho C_{v,1} V_{rel,2}^2 A = \frac{1}{2}\rho C_{v,1} A (V_w + V_r)^2 = \frac{1}{2}\rho C_{v,2} A V_w^2 \left(1 + \frac{V_r}{V_w}\right)^2 \tag{4.13}$$

where, A denotes projected area of the drums. The aerodynamic torque along the central axis is calculated as:

$$T = (F_{v,1} - F_{v,2})(d) = \frac{1}{2}\rho C_{v,1} A V_w^2 \left[C_{v,1}\left(1 - \frac{V_r}{V_w}\right)^2 - C_{v,2}\left(1 + \frac{V_r}{V_w}\right)^2\right]\left(\frac{d}{2}\right) \tag{4.14}$$

The mechanical power by the turbine can be then determined using the following equation

$$P = T\omega = \frac{1}{2}\rho C_{v,1} A V_w^2 \left[C_{v,1}\left(1 - \frac{V_r}{V_w}\right)^2 - C_{v,2}\left(1 + \frac{V_r}{V_w}\right)^2\right]\omega\left(\frac{d}{2}\right) = \frac{1}{2}\rho C_p V_w^3 A \tag{4.15}$$

The expression $\left[C_{v,1}\left(1 - \frac{V_r}{V_w}\right)^2 - C_{v,2}\left(1 + \frac{V_r}{V_w}\right)^2\right]$ is defined as power coefficient, C_p. It can be noted from equation (3.15) that the mechanical power produced by a C-section turbine is directly proportion to the total projected area by the rotor and the cube of upstream wind speed V_w (Shashank et al., 2013).

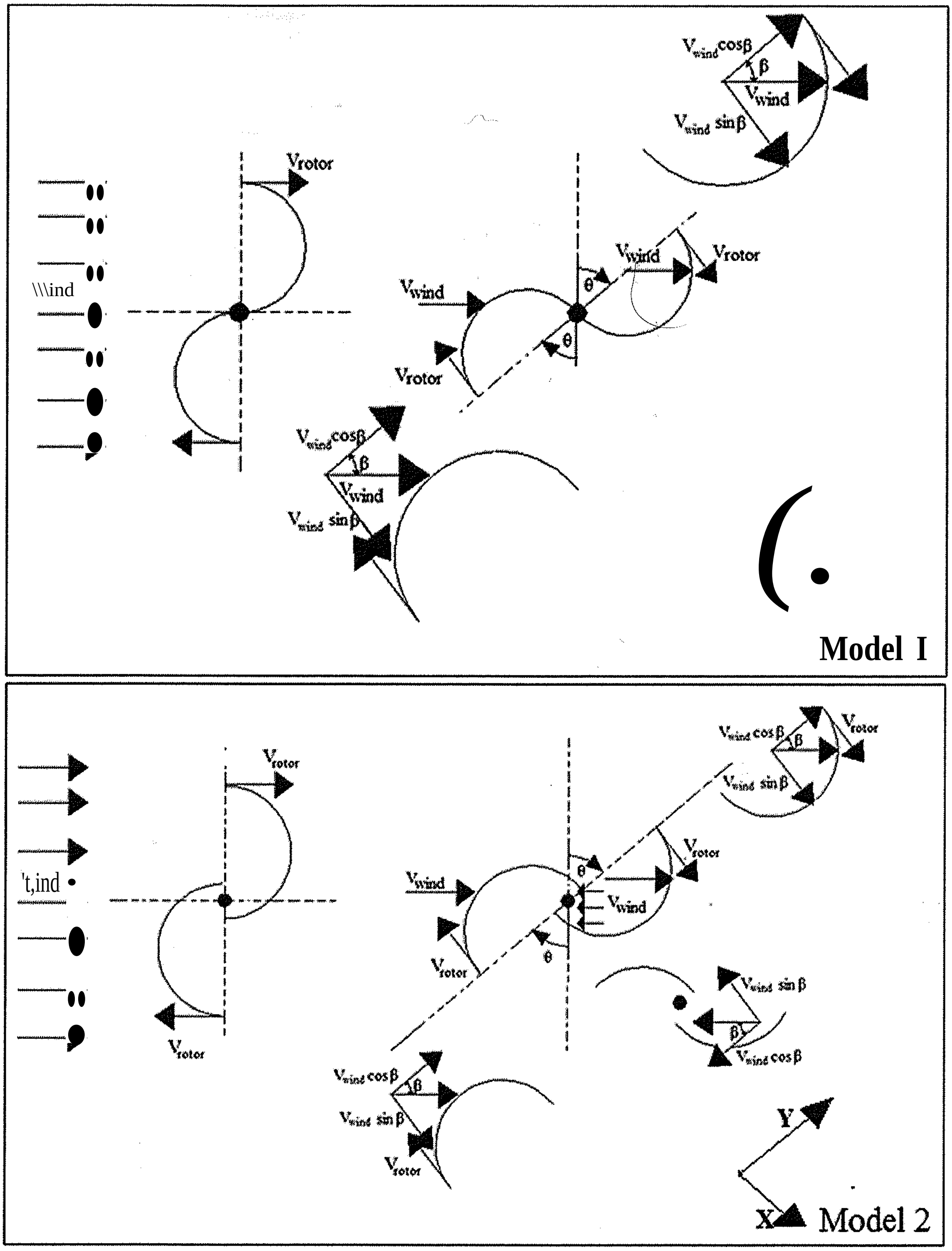

Figure 4.7: Vector Components of the Wind Speed at Savonius Rotor

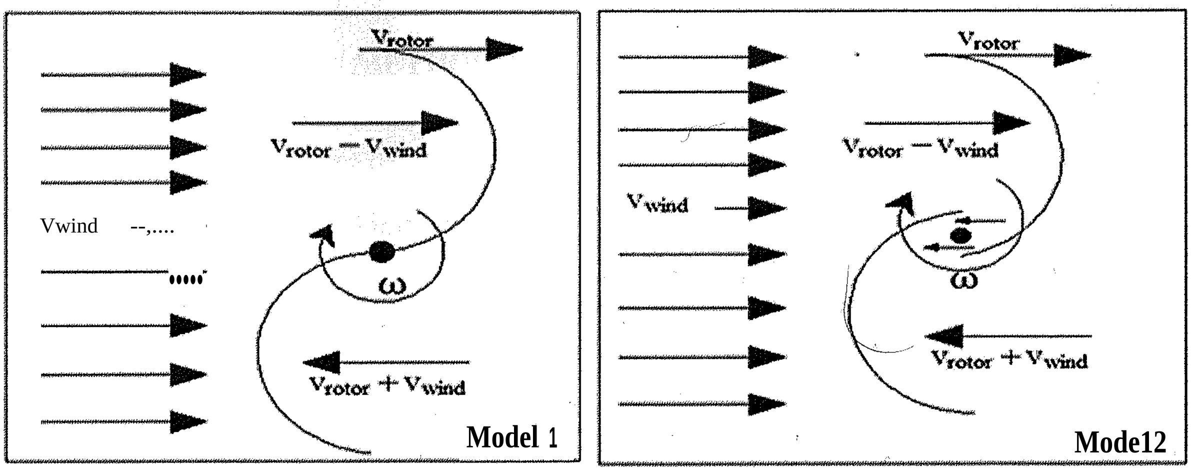

Figure4.8: Scheme of a Savonius Rotor Showing the Velocity of the Rotor and Wind Speed

CHAPTER 5
METHODOLOGY OF RESEARCH

5.1 Vertical axis Savonius Wind Turbine

The experiment used a model of Savonius vertical axis wind turbine with two, three and four blades. Figure 5.1 and 5.2 show an example of two blades Savonius vertical axis wind turbine. The shaft and blades of the Savonius rotor are made of stainless steel and PVC material, respectively. Different number of blades and smooth surface design is intended to increase the capability of wind energy capture. The Savonius vertical axis wind turbine is connected to the electromechanical dynamometer through worm gearbox to produce mechanical power, and then convert it into electricity for domestic powered generation. The turbine captures wind and moves due to the presence of drag forces, which cause it to rotate around its fixed axis as shown in Figure 5.1 and 5.2. The two dimensions, 2D, model of the Savonius rotor with different gap are Figure 5.3.The dimensions of Savonius vertical axis wind turbine model is the diameter of the blade, D, (**D** = 7, 10 and 15cm), and blade height, H, (H =30 and 50 cm) with different gap, e,(e = 0, 0.5 and lem) are shown in Table 5.1. Additionally, A floor fan is used as the wind source for doing experiments with Savonius wind turbine as shown in Figure 5.2. The wind velocity, Ues, was set at 3, 6 and 8 mis by adjusting the distance between the floor fan and Savonius wind turbine and the wind speed switch settings on the fan. to see the performance of the turbine under this controlled environment.

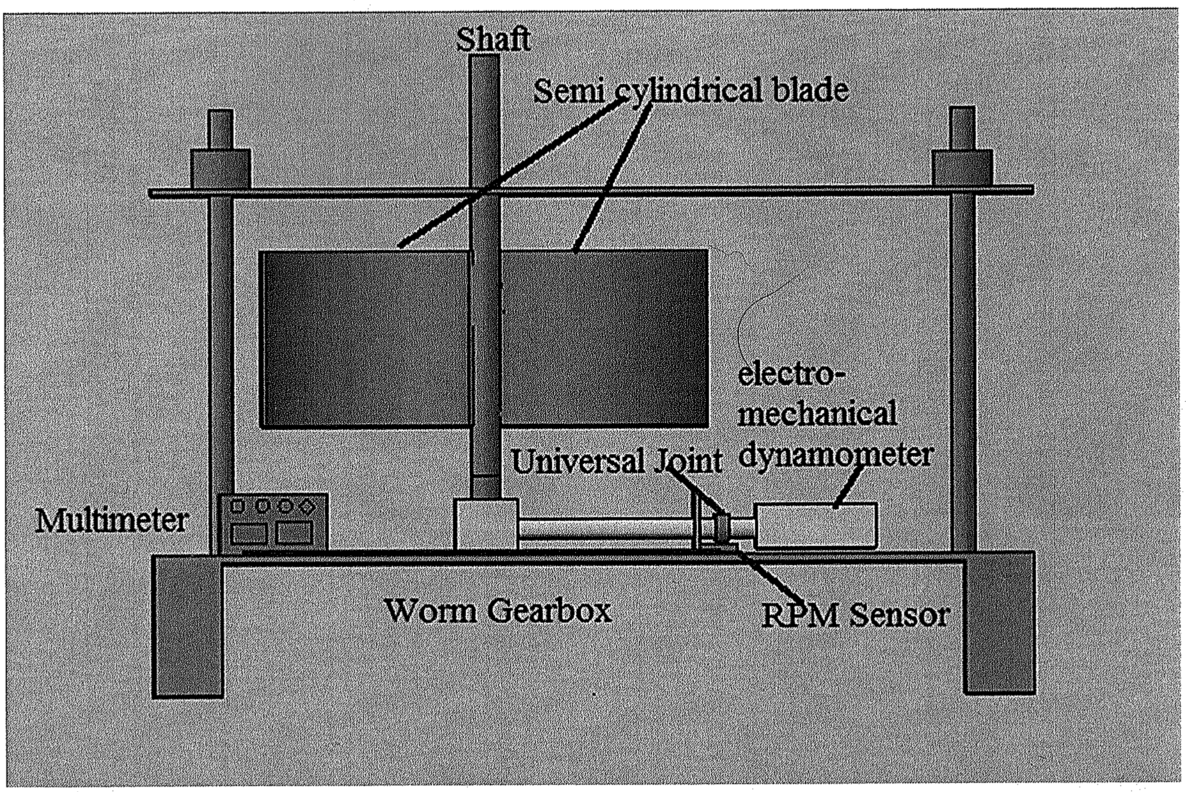

Figure 5.1: Schematic of the Experimental Setup Used to Measure Torque and Rotational Speed of the Shaft (Front View)

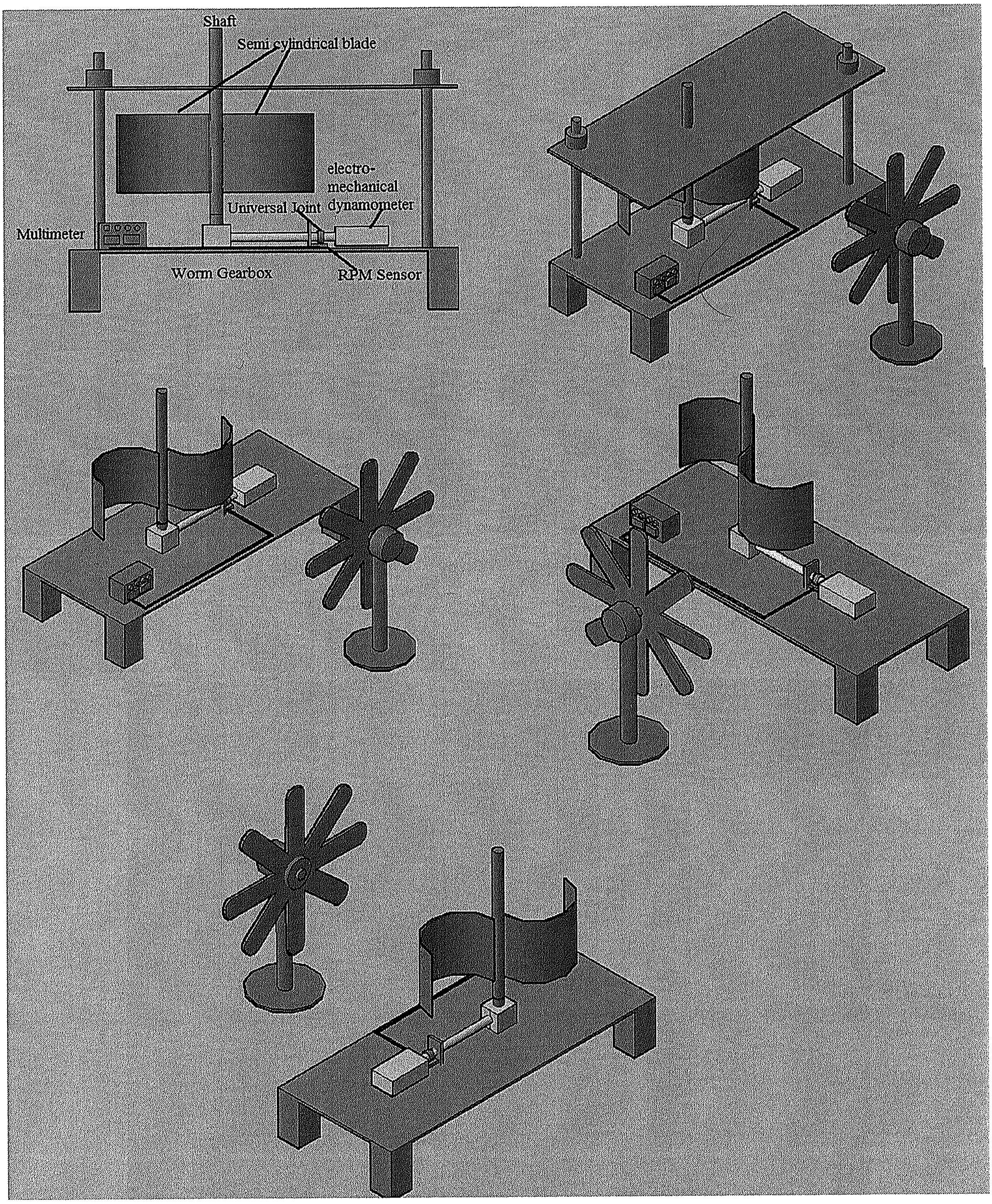

Figure 5.2: Three Dimensional Views of Experimental Setup Used to Measure Torque and Rotational Speed of the Savonius Rotor Wind Turbine

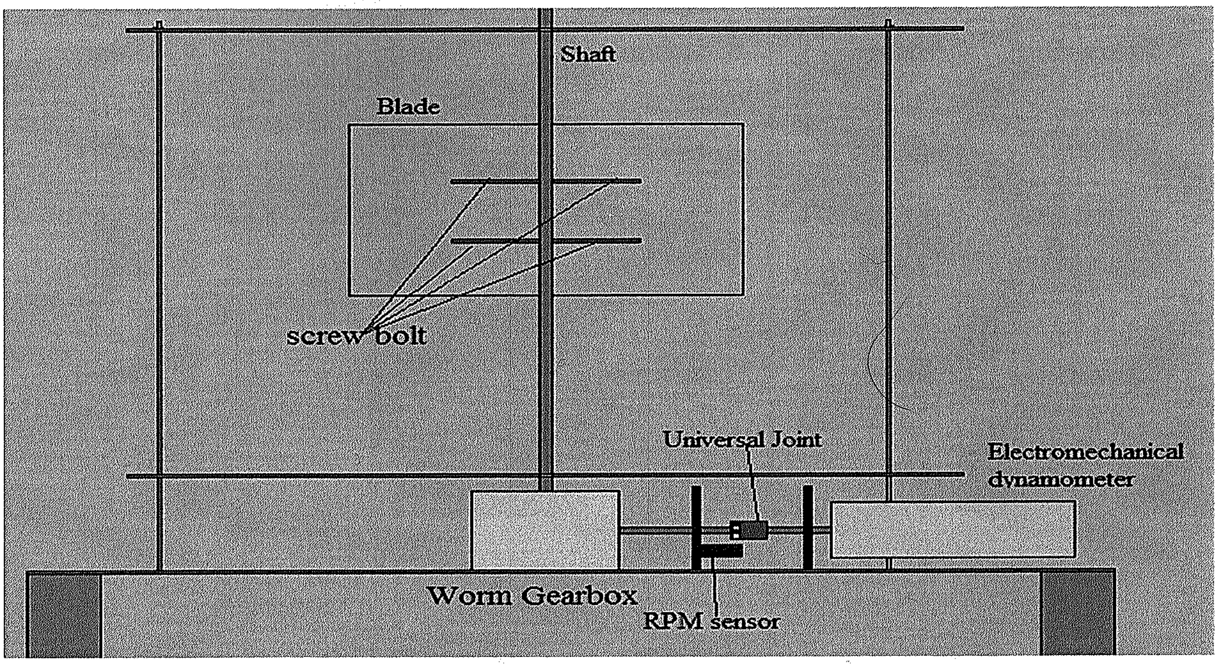

Figure 5.3: 2D-Geometry of a Savonius Rotor without Gap (e = 0cm)

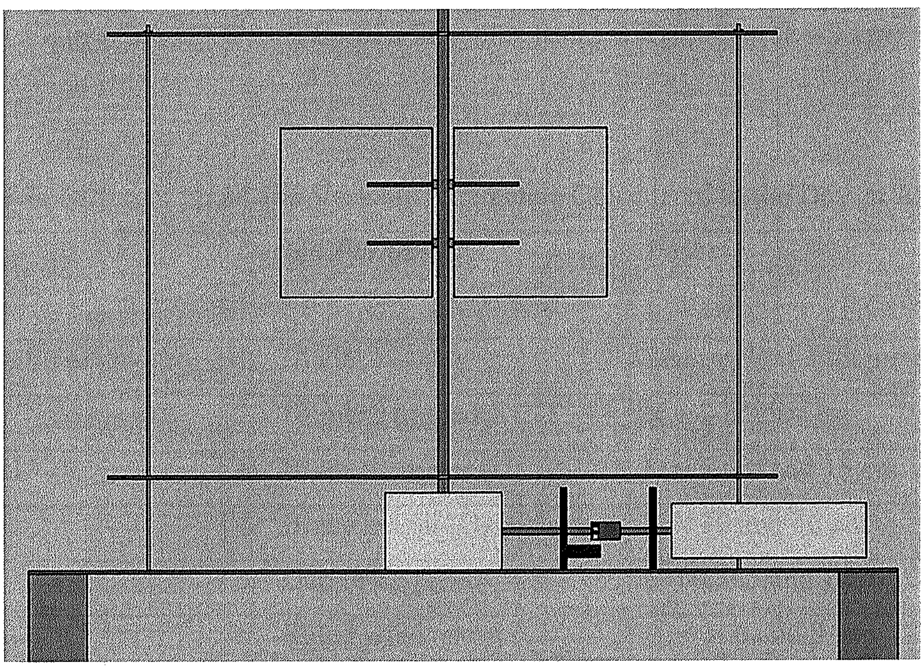

Figure 5.4: 2D-Geometry of a Savonius Rotor without Gap (e = 0.5 cm)

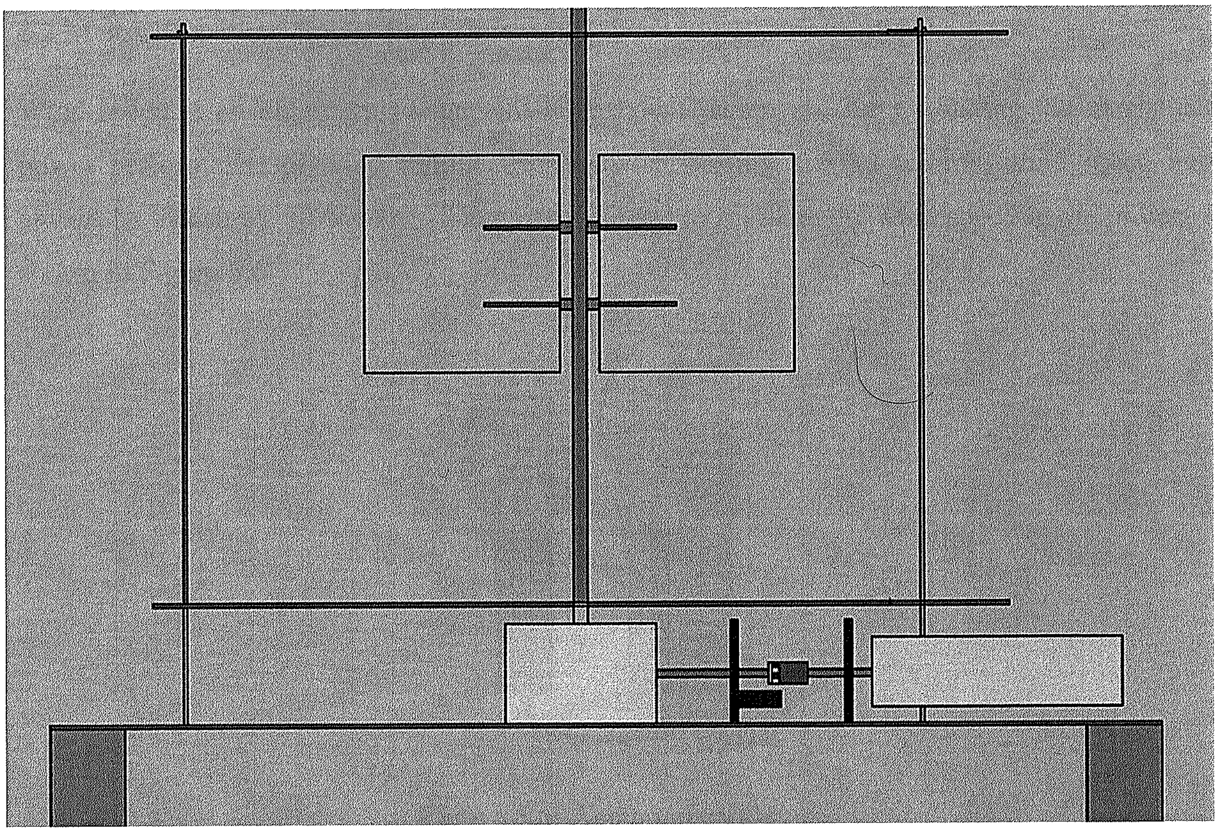

Figure 5.5: 2D-Geometry of a Savonius Rotor without Gap (e = 1 cm)

Table 5.1: Different Fixed and Variable Parameters Considered in the Design Analyses

Category	*Design Parameter*	*Value*
Physical Features	1. Blade	Semi-cylinder diameter
	2. Number of blades (N)	N = 2 blades
Dimensional	3. Blade diameter (D)	D = 7, 10 and 15 cm
	4. Blade height (H)	H = 30 and 40 cm
	5. Gap (e)	e = 0, 0.5 and 1 cm
Operational	6. Rated wind speed (U_{∞})	U_{∞}= 3, 6 and 8 m/s

5.2 Measuring Wind Spff P,iJ,l:;perimentally

Wind speed is an important parameter, independent parameter, for evaluating the mechanical power performance of wi11cl. tμrbi11e. Hence, when testing a wind turbine, wind speed must always be measured. How~-yçr).Anemometryis used to measure the wi1f~ speed in the project as shown in Figure 5.6.

Figure 5.6: Anemometry Device

5.3 Worm Gear

Gears can be used to change the direction or speed of movement. In this project, Worm gear is used for transmitting power between two non-parallel, non-intersecting shaft (see Figure 5.1 and 5.2).Worm gears involve one wheel gear (a pinion) and one shaft with a screw thread wrapped around it as shown in Figure 5.7. Worm gears change the direction of motion as well as the speed.Worm gear efficiency varies significantly when lead angle, friction factor and gear ratio changes and worm gear efficiencies range from 50% to 90%.

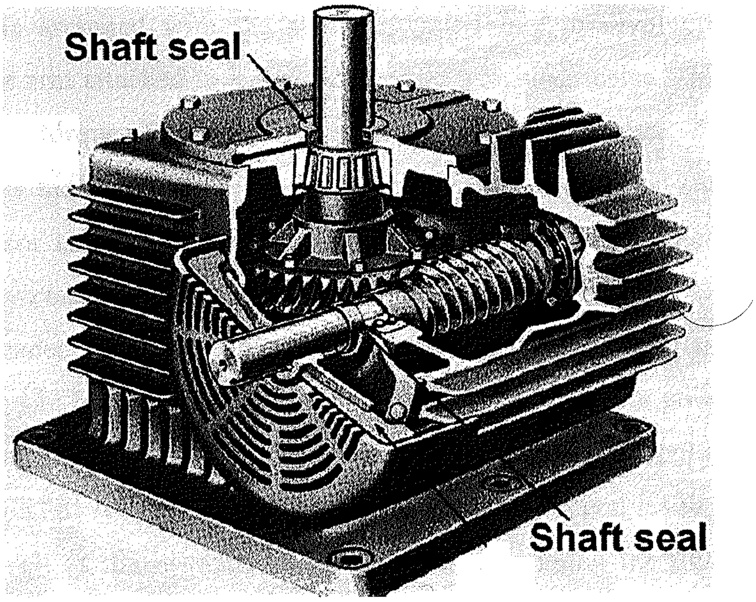

Figure 5.7: The Cut Section of a Worm Gearbox

5.4 Measuring the Torque of Vertical Axis Wind Turbine Experimentally

The procedure for measuring the torque and mechanical power of the Savonius wind turbine, the first step is to build the turbines with the different sizes. This was done using PVC material for the blade (Semi-cylinder shape) of 0.5 mm thick with different height and diameter as shown in Table 5.1. The shaft of the Savonius rotor is made from stainless steel with 2 cm diameter and 1 m long. The finished turbine was then attached to a worm gearbox (Worm gear is used for transmitting power between two non-intersecting shaft), which was attached to electromechanical dynamometer and was placed in front of a floor fan. Electromechanical dynamometer is used to measure force and torque from a rotating shaft of Savonius vertical axis wind turbine as shown in Figure 5.1 and 5.2. The electromechanical dynamometer system is consisted water level, arms, weight and balance weight for measuring the output torque of wind as shown in Figure 5.8. Also, it consists of a direct current (DC) machine with the stator cradle-mounted on anti-friction bearings. The rotor is connected to the shaft of the machine under test. The stator is constrained from rotating by a radial arm of known length to which is attached a scale for measuring the force required to prevent rotation. Torque is described as a force acting along a distance. Torque is something that creates twisting and tries to make something rotate.The turbine is arranged with the stator mounted free to revolve but restrained from revolving by a brake arm attached to it and fastened to weighing scales. The force, F, shown on the scales becomes a torque, T, when multiplied by the lever distance, d, from the centre of rotation. Power, P, is measured as the torque operating at the rotational speed of the generator shaft. The RPM sensor is used to measure the rotational speed of the shaft which was placed under the special universal joint as shown in Figure 5.1 and 5.2.This RPM sensor is cô~"d to multimeter device reader. However, the multimeter device reader is device used to read the RPM of the shaft as shown in Figure 5.2. The floor fan was turned into low power and adjusting the distance between the floor fan and Savonius wind turbine, where it would be emitting a wind speed of 5 *mis.* The RPM reading on the multimeter and wind speed result on the Anemometry were recorded, as well as the distance and weight for calculating the torque of the Savonius turbine. Then, floor fan is turned to medium and high power, and recorded the same data. The same method is used to make and test the other turbines, and recorded the same data.

The formula for torque and power are:

$$T = F \times d \qquad [N.m] \qquad (5.1)$$

$$P = T \times w \qquad [Watt] \qquad (5.2)$$

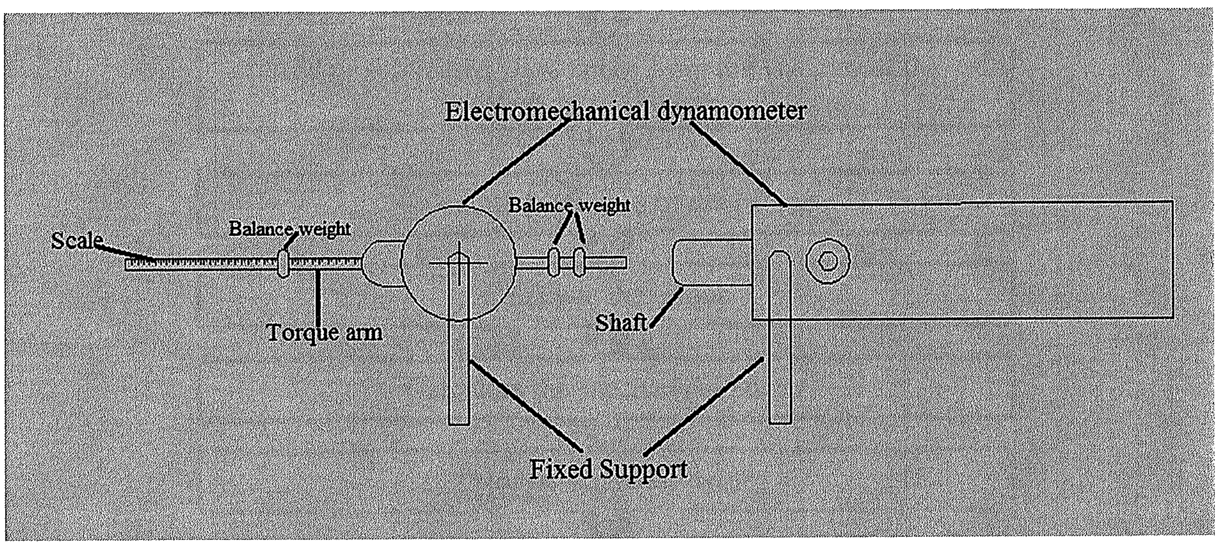

Figure 5.8: Scheme of Electromechanical Dynamometer (Front and Right Views) Showing the Components of Electromechanical Dynamometer

5.5 Theoretical Procedures for Calculating the Mechanical Power

As mentioned in the previous chapter, the procedures of power calculation of Savonius vertical axis wind turbine can be described as the following steps and shown in Figure 5.9:

1. Analysis the velocity component into X-axis and Y-axis which depends on the position of the blade as shown in Figure 4.7.
2. Add or subtracted wind speed from the velocity of the Savonius rotor which depends on the direction of the velocity X-component (see Figure 4.8).
3. Find out the values of the drag coefficient, C_D, which depends on the position of the blade.
4. Calculate the values of drag force, F_D, (pressure force) for two, third and fourth blade (the blades are different by 180°, 120° and 90°from each other respectively).
5. Calculate the torque, T, for each blade (Eq. 5.1)
6. Calculate the total values of torque of this rotor for the preparation of Mechanical power calculation (Eq.5.2)
7. Calculate the average torque for the preparation of average Mechanical power calculation.

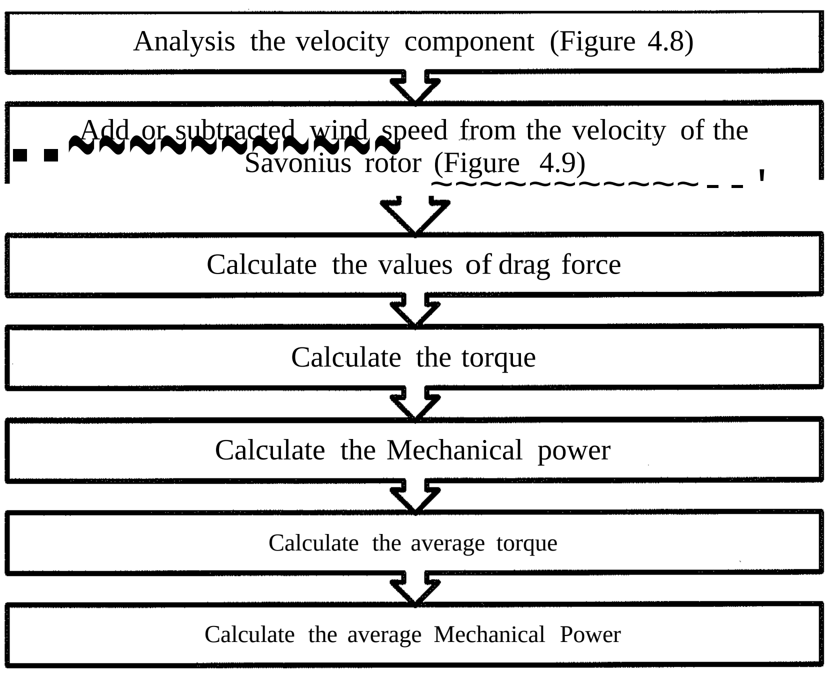

Figure 5.9: Procedure for Calculating Mechanical Power of Savonius Rotor

CHAPTER6

RESULTS AND DISCUSSIONS

6.1 Comparison of Theoretical and Experimental Torque of Classic Savonius Wind Turbine Rotor (2 Blades)

Before applying the theoretical study in Savonius wind turbine, a comparative study has be~_/ done between the theoretical study with Ali (2013) by using the same dimension of Savonius wind turbine, wind speed and angular rotation. The blade of a Savonius wind turbine was made of semi-cylindrical scoops of diameter (d = 100 mm), height of (H = 200 mm) and thickness of (0.079 mm) as shown in Figure 3.7. The theoretical was compared with the experimental data which obtained from an article Ali (2013). at wind speed 5.3 *mis* and 458 RPM. Figure 6.1 and Table 6.1 shows the comparison between experimental and theoretical predictions data torque of the Savinous wind turbine rotor. Also, the percentage error between them is shown in Table 5.2. As can seen, the percentage error between the theoretical predictions and experimental data at 0°, 90°, 150°, 180°, 270°, 330°, 360° is zero percent. Whereas, at 30°, 60°, 120°, 210°, 250°, 300° the percentage error between the experimental and theoretical data is in the range between 13 and 30 percent.

Table 6.1: Comparisonib~tw'e.en.füe Experimental and Pervious Study Torque of Savonius Wind Turbine Rotor

	Torque [N.m]		
Rotor angle [0J	Experimental data	Theoretical data	Absolute Error [%]
0	0.039	0.039	0
30	0.058	0.056	3.5
60	0.038	0.057	33.3
90	0.02	0.02	0
120	0.015	0.013	15.3
150	0.009	0.009	0
180	0.039	0.039	0
210	0.058	0.056	3.5
250	0.038	0.057	33.3
270	0.02	0.02	0
300	0.015	0.013	15.3
330	0.009	0.009	0
360	0.039	0.039	0

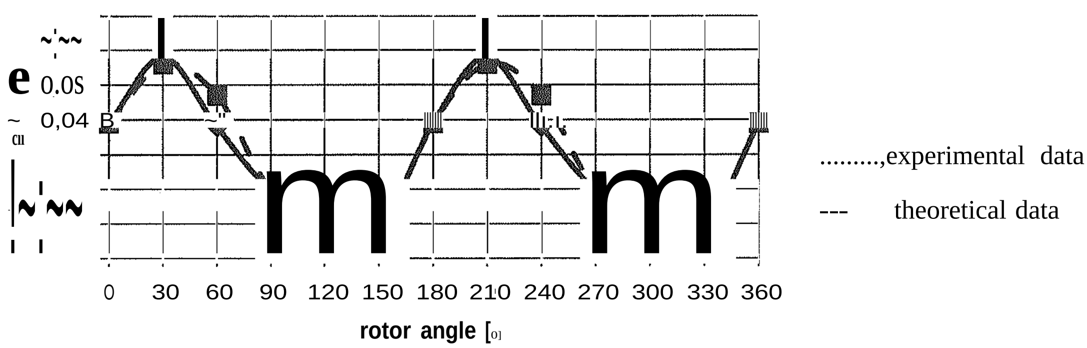

Figure 6.1: Percentage Error between the Experimental and Prediction Data with Rotor Angle of Savonius Wind Turbine Rotor

6.2 Theoretical Results.of.'l.'orque of Savonius Rotor

As mentioned previôüşly, Torque and mechanical power of the Savonius rotor were calculated for varying sizes ofblıιqt,ş ıı1ld varying gap.

Figures 6.2, 6.3 andi6.4(show the torque varies with the change in rotor angle .for different number of wind speed (3, 6 and 8 mis), gap (O and 0.5 cm) and blade diameter (7, 10 and 15cm) with fixed blade height (30 cm) şvhich were chosen randomly. It can be observed·,that,the torque is rapidly increasing with thesincrease in wind speed and blade diameter.

It can be noticed from Figures 6.3 and 6.4 that the torque of the Savonius wind turbine starts to increase from (0° to 30°) to reach its maximum value and then goes down to decrease from (30° to 150°) to reach its lowest value. It is noticeable that torque values are yielding the symmetry for flow angles higher than (180° to 360°). While in Figure 6.2, it goes down to decrease from (30° to 120°) to.reach its lowest value, then it increases from (120° to 150°) to reach till reach the torque value of rotor angle 0°. Then torque values are yielding the symmetry for flow angles higher than (180° to 360°).

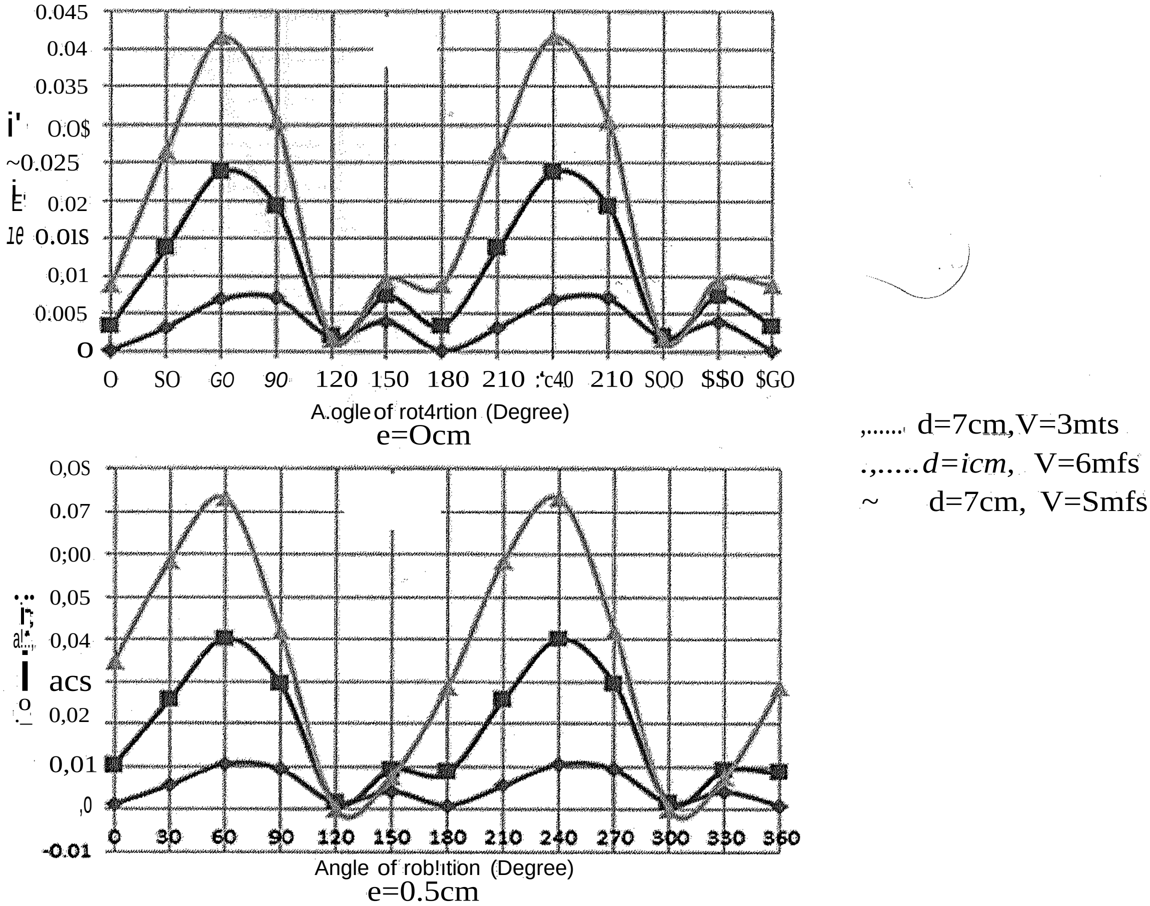

Figure 6.2: Torque of Savonius Turbine Various Rotor Angle with Different Wind Speed (V = 3, 6 and 8m/s) and Fixed H = 30 cm and d =7cm

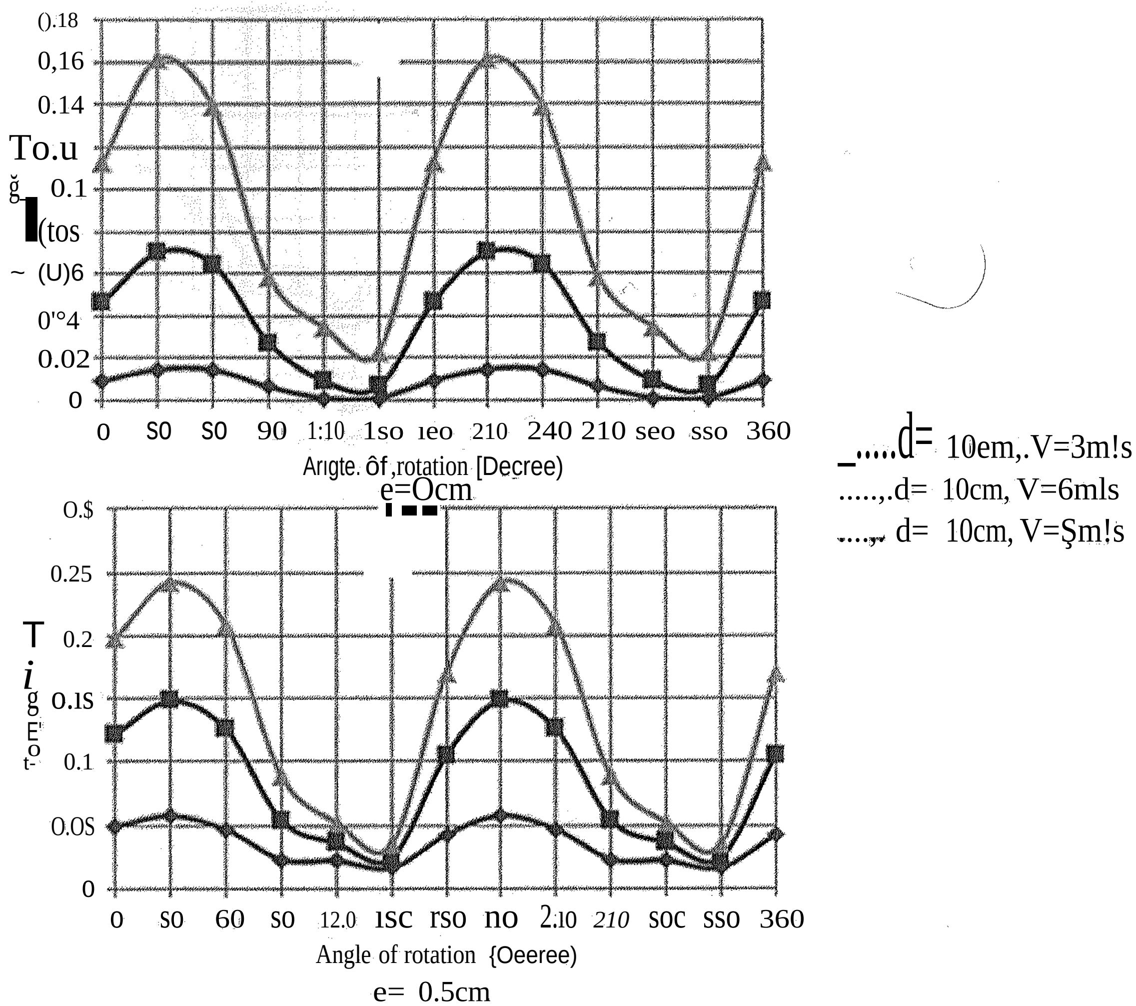

Figure 6.3: Torque of Savonius Turbine Various Rotor Angle with Different Wind Speed (V = 3, 6 and 8m/s) and Fixed H = 30 cm and d =10 cm

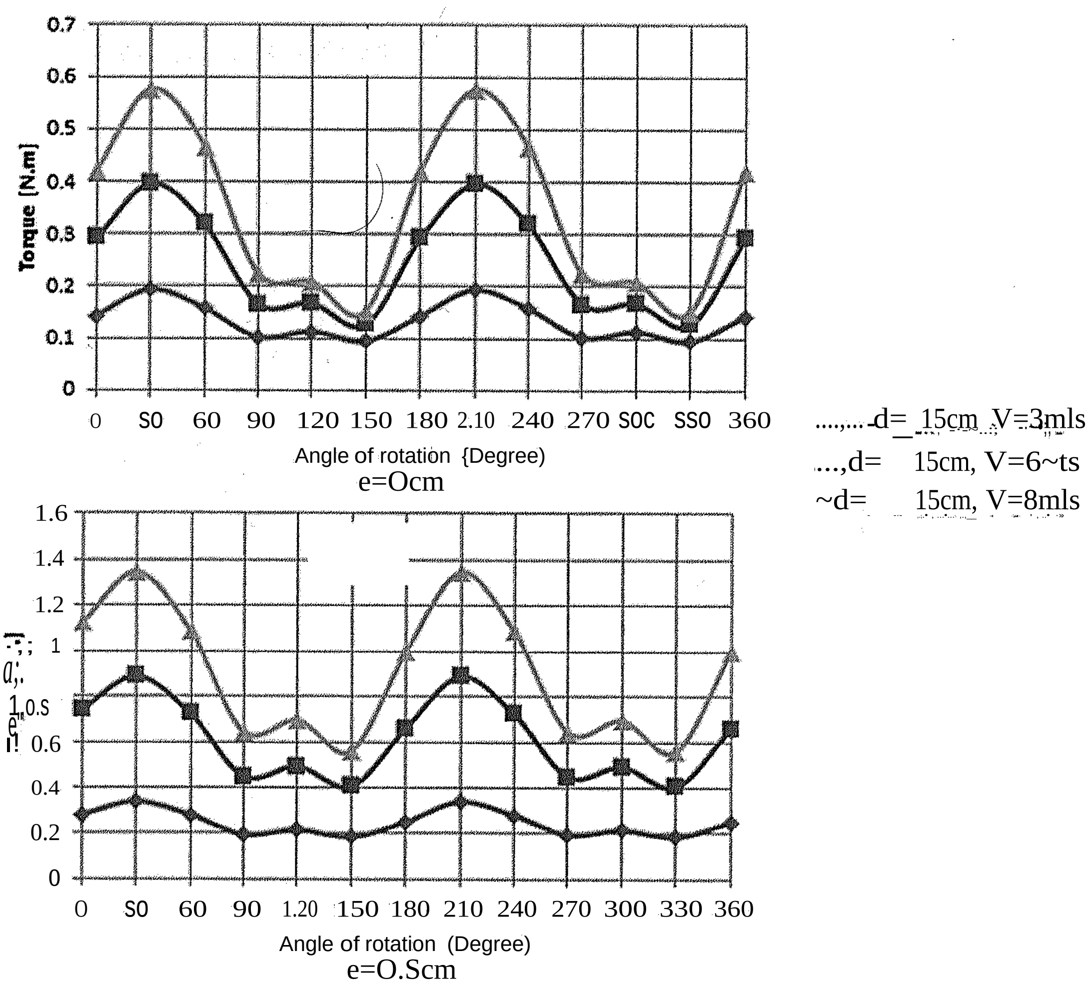

Figure 6.4: Torque of Savonius Turbine Various Rotor Angle with Different Wind Speed (V = 3, 6 and 8m/s) and Fixed H = 30 cm and d =15 cm

Figure 6.5 illustrated the amount of torque produced from a different gap of Savonius wind turbine rotor with constant wind speed, angular rotation and blade size. In this case, it shows the effect of the gap on the torque of the Savonius wind turbine. It is observed that the increasing gap leads to increase the torque of the Savonius wind rotor. Also, Figure 6.6 shows the effect of blade height on the torque of wind turbine. It shows that the torque of Savonius wind turbine increases when the blade height increases with constant wind speed, blade diameter and fixed gap. It was also found that the 40 cm height blade turbine produced double the torque of 30cm height bladed turbine.

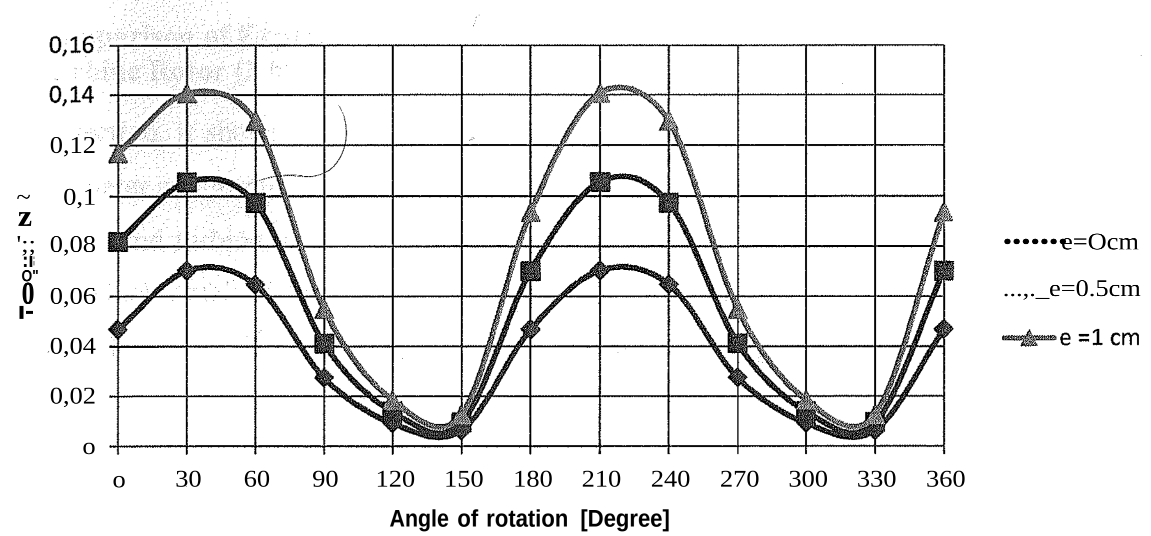

Figure 6.5: Torque of Savonius Turbine Various Rotor Angle with Different Gap (e = 0, 0.5 and lem) and Fixed H = 30 cm and d =10 cm, V = 6 *mis* and 450 RPM

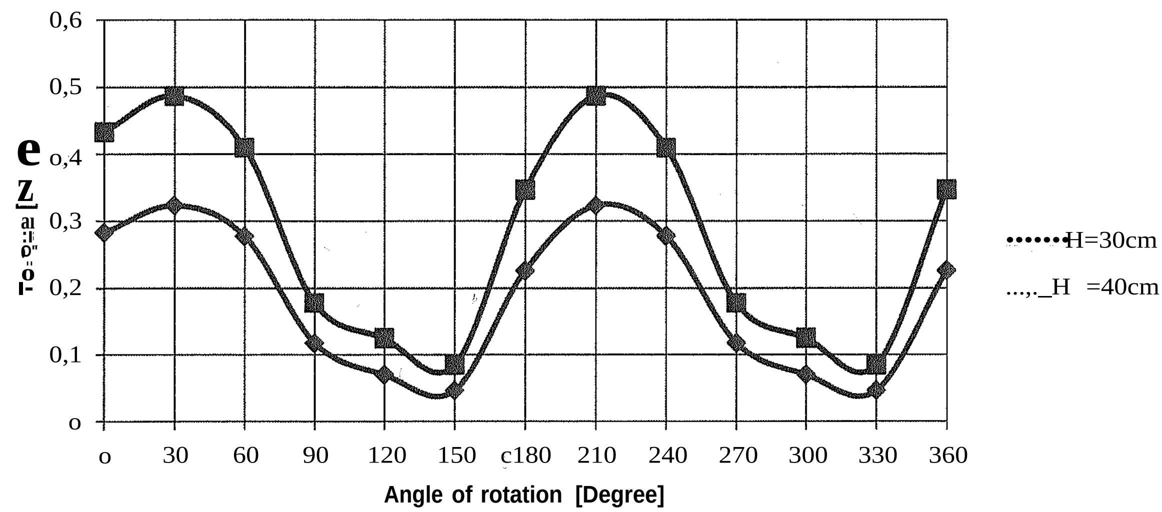

Figure 6.6: Torque of Savonius Turbine Various Rotor Angle with Different Blade Height (H =30 and 40 cm) and Fixed e = 0 cm and d =10 cm, V = 8 *mis*

6.3 **Comparison of Experimental** and Pervious Study Torque of Classic Savonius Wind **Turbine Rotor (2 blades)**

In this section, it shows the difference the torque value, which measured by electromechanical dynamometer and torque value, which obtained from Ali (2013) by using the same dimension of Savonius wind turbine, and wind speed as shown in Table 6.2. The blade of a Savonius wind turbine, which obtained from Ali (201J) was made of semi-cylindrical scoops of diameter (d = 100 mm), height of (H = 200 mm) and thickness of (0.079 mm). While the blade of a Savonius wind turbine of this work was made from PVC material. It is noticed that percentage error between both values of RPM and torque is about 20 percent.

Table 6.2:. Comparison between the experimental and pervious study torque of Savonius wind Turbine rotor

Pervious Study		
Wind velocity [m/s]	RPM	Torque [N.m]
5.3	485	0.030385
Experiment		
Wind velocity [m/s]	RPM	Torque [N.m]
5.3	400	0.0375

6.4 Relationship between Rotor Speed and Wind Speed with Variable Blade Size and Gap

Figure 6.7, 6.8and 6.8 show the variation of RPM with wind speed of the Savonius wind turbine. It shows that for a constant blade diameter and different blade height and gap, the rotor speed, RPM, is proportional to wind speed. However, increasing the wind speed, blade size and gap lead to an increase the rotor speed of the Savonius wind turbine.

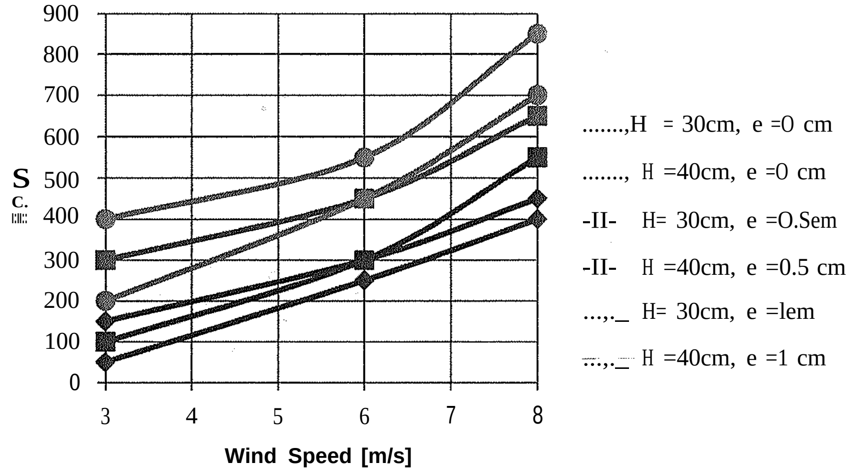

Figure 6.7: RPM versus Wind Speed for Different Blade Height and Gap with a Fixed Blade Diameter, d = 7cm

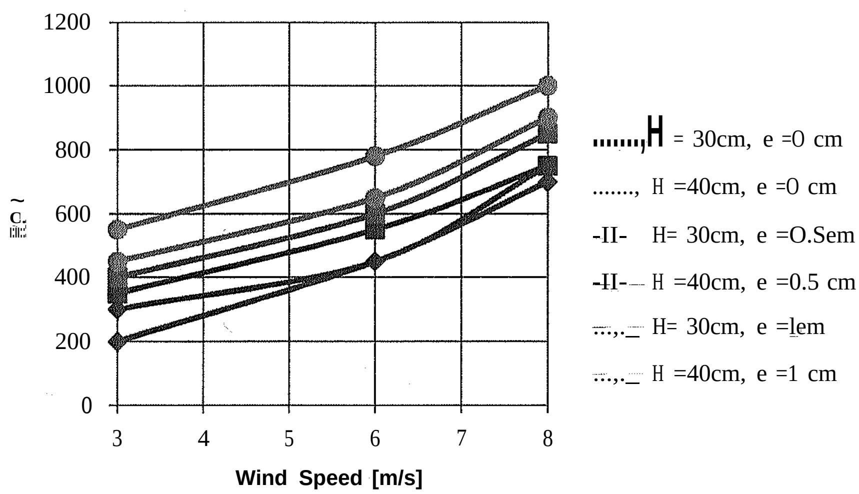

Figure 6.8: RPM versus Wind Speed for Different Blade Height and Gap with a Fixed Blade Diameter, d = 10cm

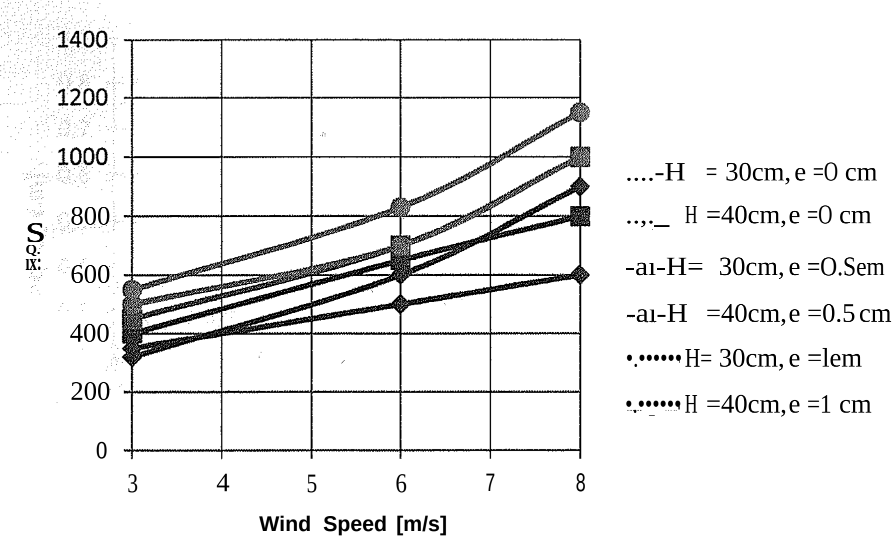

Figure 6.9: RPM versus Wind Speed for Different Blade Height and Gap with a Fixed Blade Diameter, d = 15cm

6.5 Relationship between Torque and Wind Speed With Variable Blade Size And Gap

As observed in Figure 6.10 to 6.12, Torque increases with increasing wind speed, blade diameter, blade blade height and gap. It can be noticed that the torque is increased proportional to wind speed, blade size and gap as shown in Figure 6.10 to 6.12.

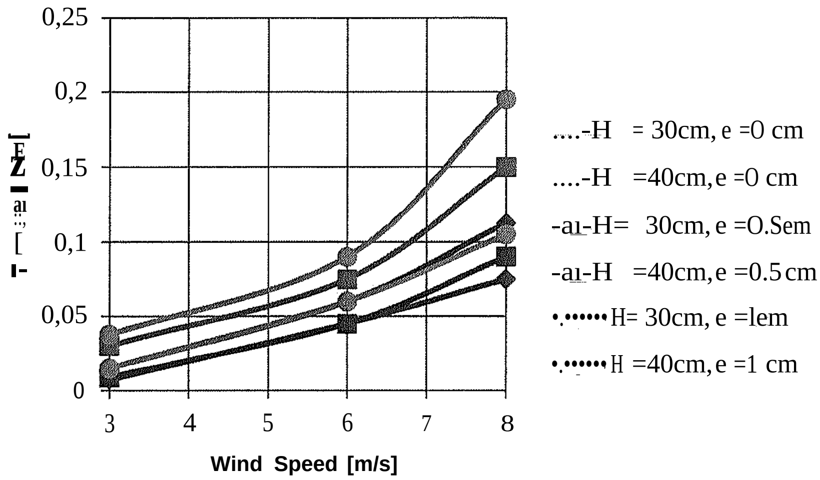

Figure 6.10: Torque versus Wind Speed for Different Blade Height and Gap with Constant Blade Diameter, d = 7cm

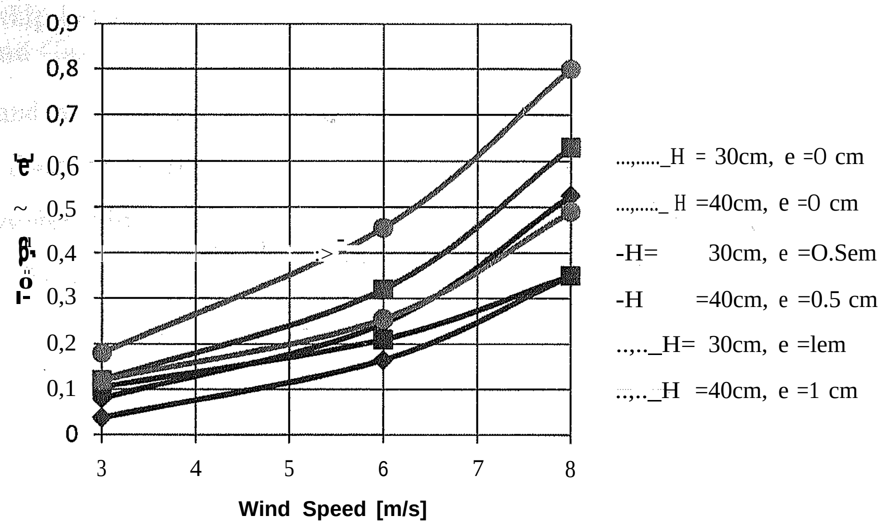

Figure 6.11: Torque versus Wind Speed for Different Blade Height and Gap with Constant Blade Diameter, d = 10cm

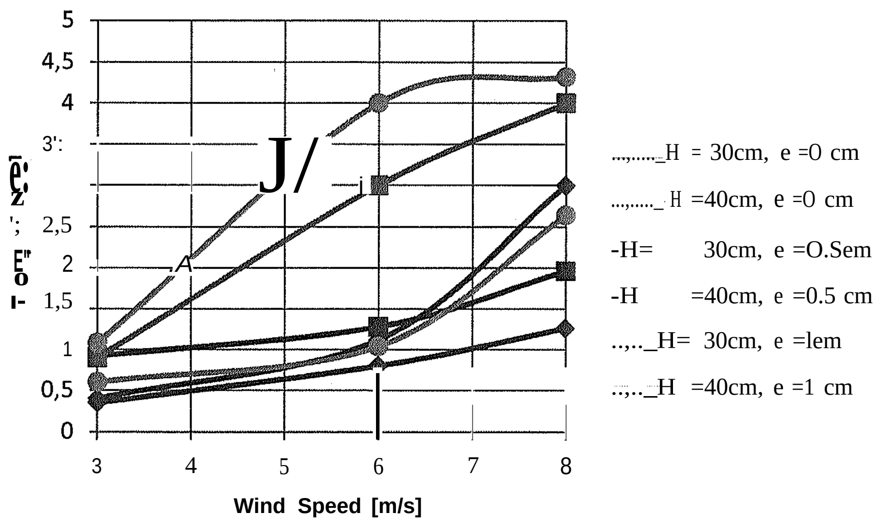

Figure 6.12: Torque versus Wind Speed for Different Blade Height and Gap with Constant Blade Diameter, d = 10cm

6.6 Relationship between Torque and Blade Diameter with Variable Wind Speed, Blade Height and Gap

Figure 6.13 and 6.14 shows the relationship between the Torque and blade diameter and gap, respectively. From these figures, the increase in blade diameter and gap lead to increase the torque of Savonius wind turbine. It is also revealed that as the blade diameter and gap increase, the torque of the Savonius wind rotor increases in a linear fashion. Additionally, the torque is rapidly increasing with the increase in blade diameter and gap.

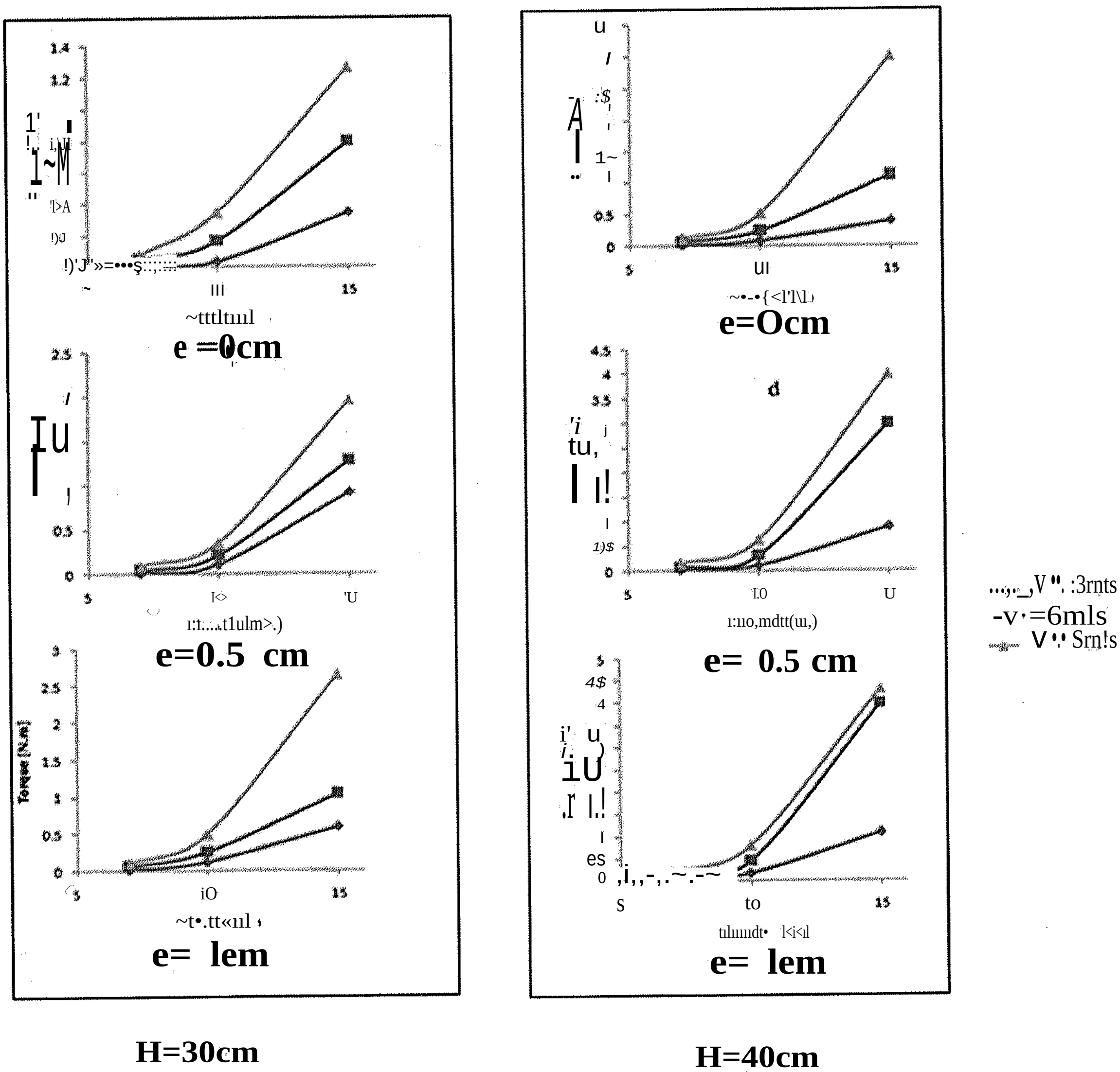

Figure 6.13: Torque versus Blade Diameter for Different Blade Height, Wind Speed and Gap

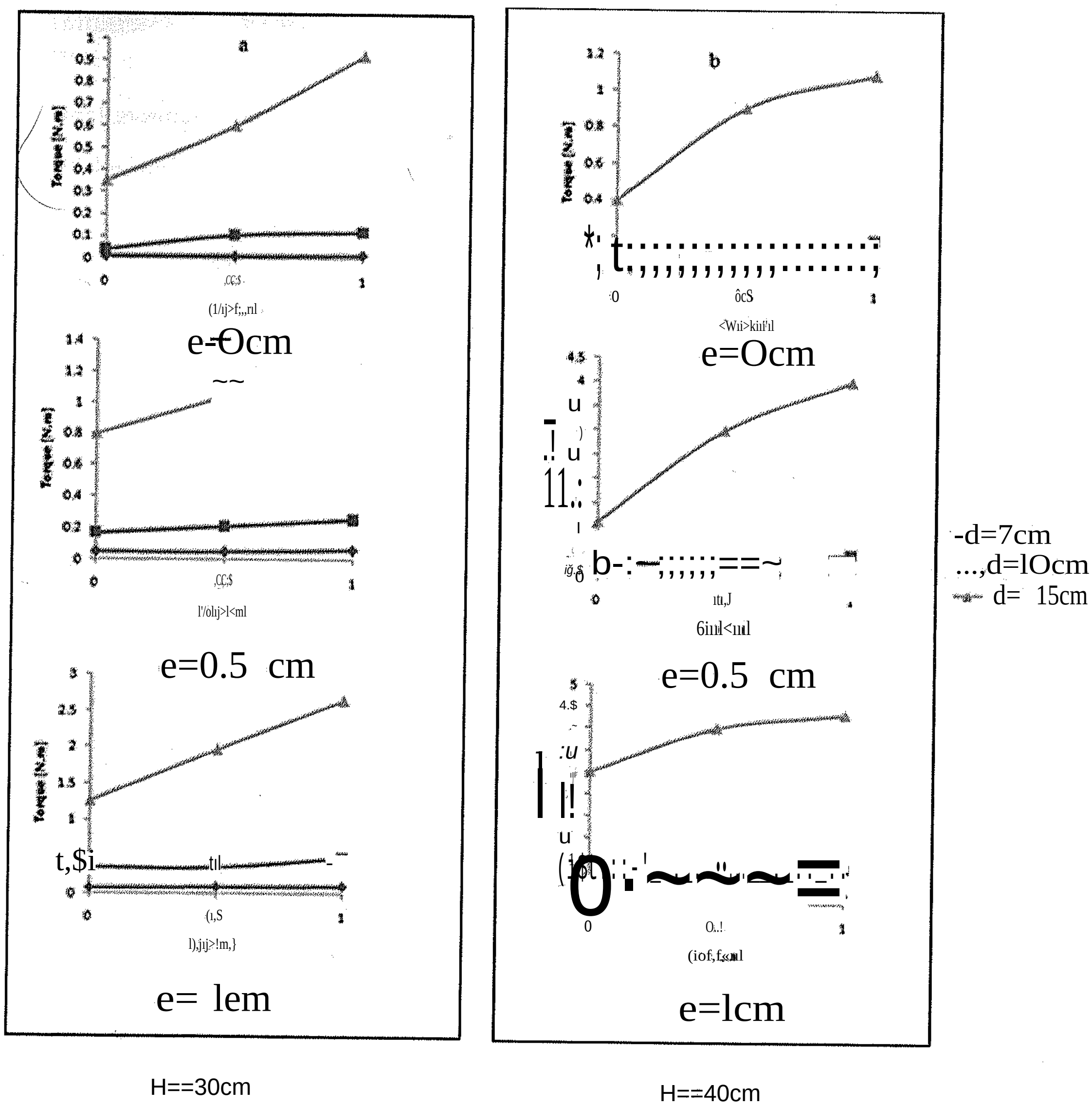

Figure 6.14: Torque versus Gap for Different Blade Height, Blade Diameter Wind Speed

6.6 Comparjsmr()f'fheoretical study and Experimental Torque of Savonius Wind Turbine Rotor

Tlieoretical.a.yer~gy.J()I"que, traditionally, average torque is calculated by dividing the sum of all {1ues of theoreticaltorque at a different rotor angle by a number of the values. It is given by the formula

$$T_{average} = \frac{\sum_{i=1}^{n} T_i}{n} \tag{6.1}$$

Figures 6.15 and 6.16 illustrate the amount of theoretical average torque produced from the Savonius wind turbine rotor with different size at the different wind speed and RPM, respectively. Additionally, the comparison between the theoretical result and experimentaltorque are shownin Figures6.15 and 6.16. It can notice that the torque, Theoretical and experimental, is rapidly increasing with the increase in the size of the blades, gap and wind speed. The absolute error between them is between the range 0 and 17% as shown in Figures. However, from these Figures, it is clear that as the blade size, gap and wind speed increase, the torque of the Savonius rotor wind turbine will increase.

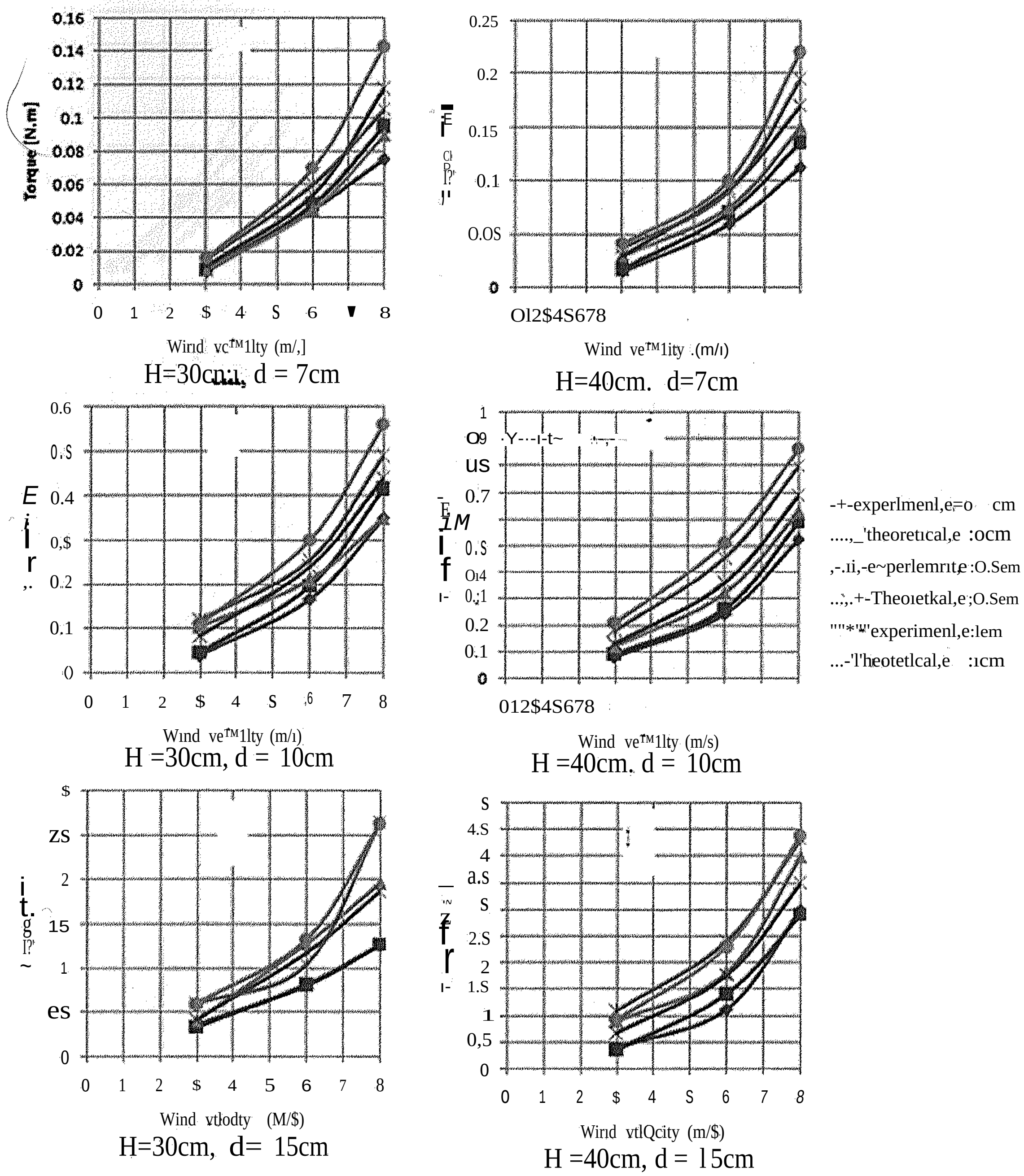

Figure 6.15: Torque versus Wind Speed for Different Gap and Blade Size

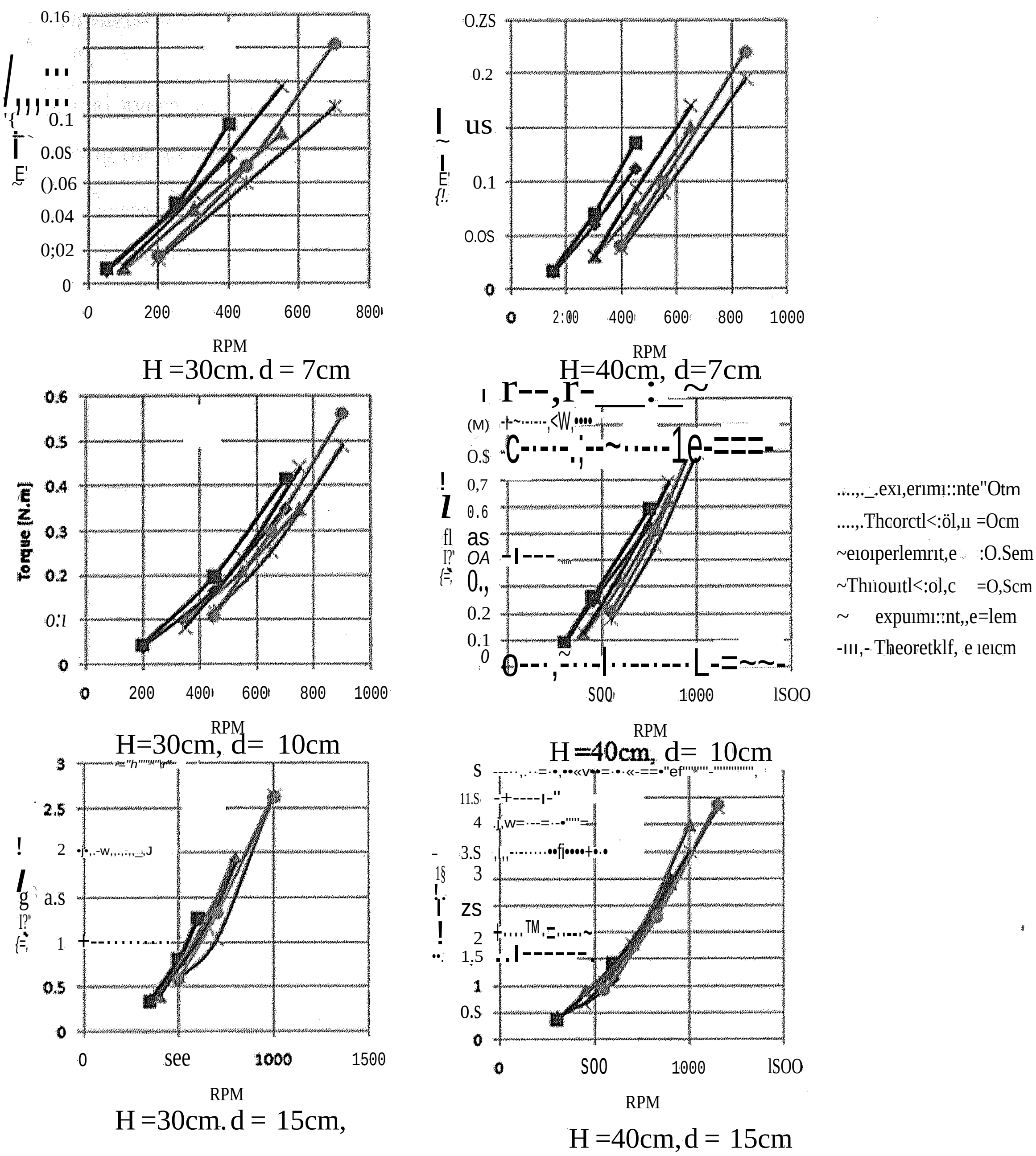

Figure 6.16: Torque versus RPM for Different Gap and Blade Size

6.7 Compal'jsonof Theoretical study and Experimental Powel' of Savonius Wind Turbine (Rotol'

Tlıs!?retic;ıv:age Mechanical power.ıtraditionally average mechanical power is calculated by multiplying the average torque by angular speed, rotor speed,. It is given by the formula

$$P_{average} = T_{average} \times W \tag{6.2}$$

Figures 6.17 and 6.18 illustrate the relationship between the average of theoretical mechanical power and experimental mechanical power and size of blades and gap with variable wind speed and RPM, respectively. Additionally, it is observed that the absolute error between them is between the range 0 and 17% as shown from these Figures. However, from these figures, it is clear that as the blade size, gap and wind speed increase, the Savonius rotor wind turbine will produce more mechanical power.

It can notice from the figures that a greater number of blades increase the weight to be turned by the turbine. On the other hand, more blades provide a greater available surface area for the wind to push, so it would produce more turning power. Having fewer blades could be beneficial because it will not be as heavy, and will be easier to tum than a greater number of blades, but it will also be somewhat inefficient because it produces less turning power.

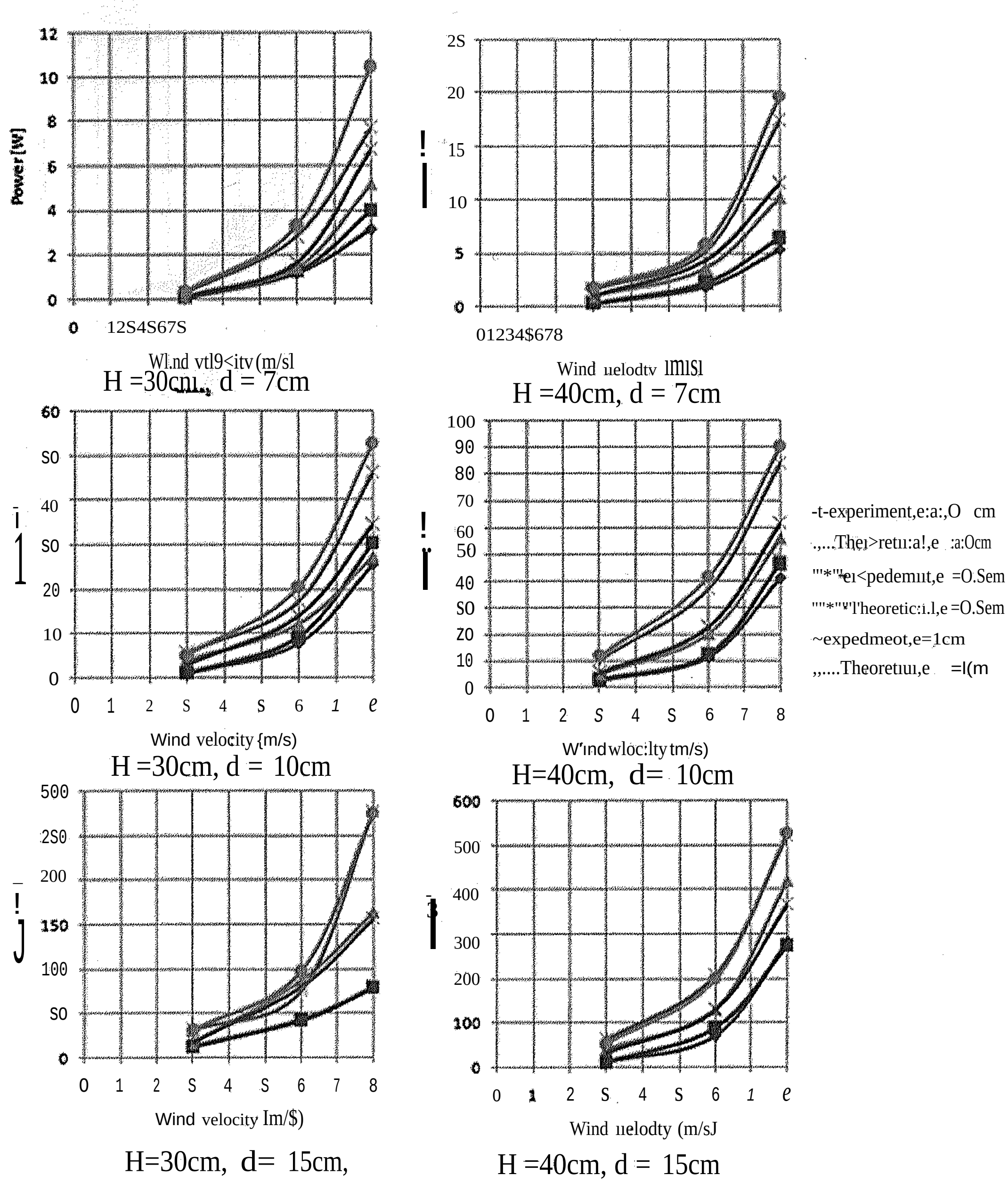

Figure 6.17: Power versus Wind Speed for Different Gap and Blade Size

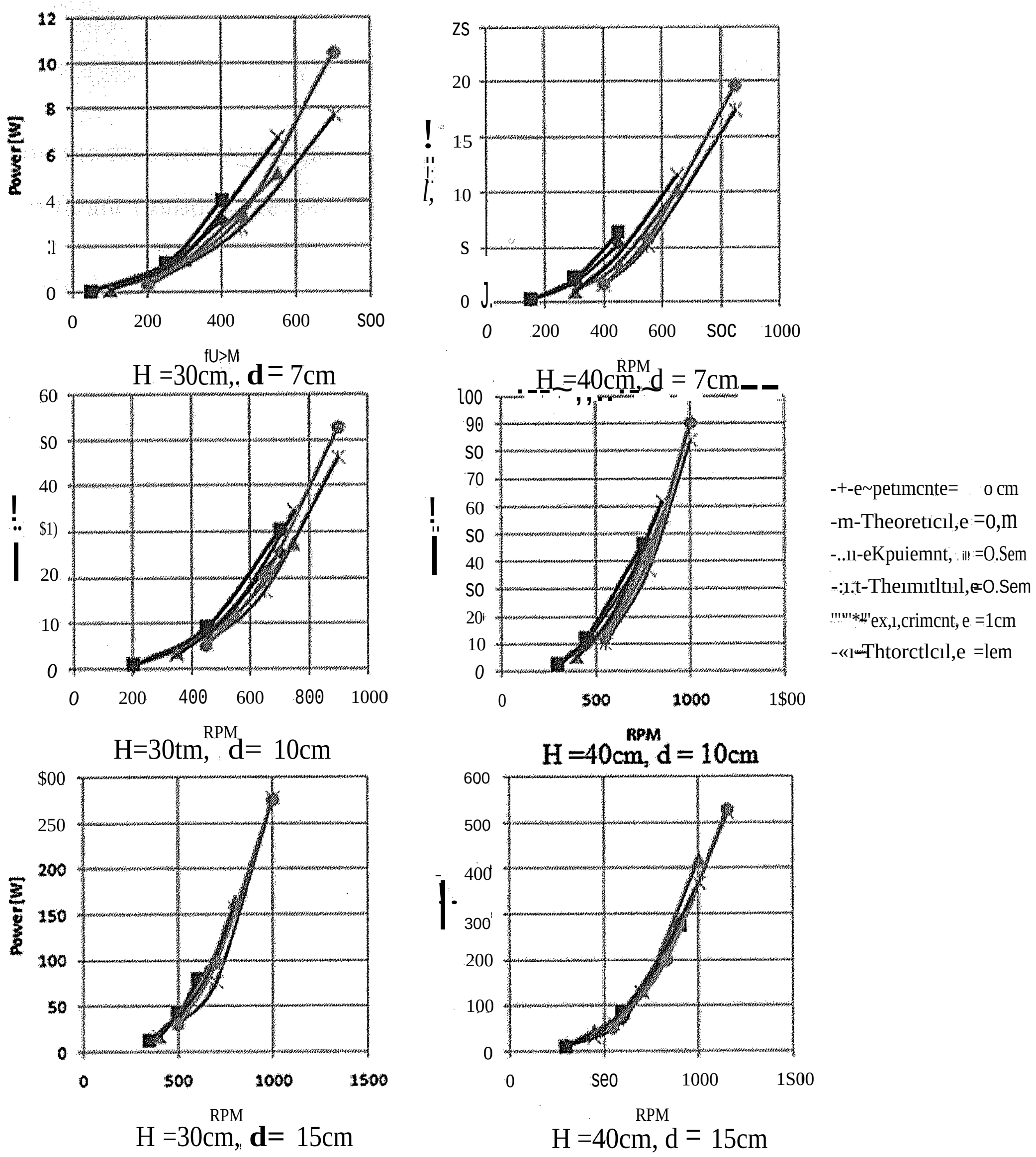

Figure 6.18: Power versus RPM for Different Gap and Blade Size

CHAPTER 7

CONCLUSION AND FUTURE WORK

Based on the research work, the aims and objections of the research project have been achieved. The significant findings are summarized below.

7.1 Conclusion

In conclusion of this study, the objectives which were to design a simple Savonius wind turbine and compare the experimental result with the theoretical result, by using velocity analysis based on some literature reviews done from several of previous researches, of the mechanical power for models of the Savonius wind turbine rotor.

The torque and mechanical power of the Savonius models were calculated at different wind speed of 3, 6 and 8 *mis,* blade diameter of 7, 10 and 15 cm, gap of 0, 0.5 and lem and blade height of 30 and 40 cm. The blades of the models were made from PVC material. All tests were conducted indoors to reduce interfering wind and other elements. The same environment was used for each test

From this study, the following conclusions are summarized:

- A greater diameter of blades increases the weight to be turned by the turbine. On the other hand, increasing the blade diameter provides a greater available surface area for the wind to push, so it would produce more turning power. Having a smaller diameter blade could be beneficial because it will not be as heavy, and will be easier to tum than high diameter of blades, but it will also be somewhat inefficient because it produces less turning power.
- The study showed that the torque and mechanical power increase with increase of blade size and wind speed.
- Size of blades will influence the rotation of the rotor of Savonius wind turbine models. The blade of diameter 15 cm and height 40 cm produces higher rotational speed than other blade size.
- Increasing in blade size and wind speed lead to increase the torque and mechanical power of the Savonius wind turbine.

- Theoretical study becomes a useful study for the study of wind rotors, since it allows obtaining values for the torque and mechanical power of the wind turbine without the need for instrumentation.
- It was also found that the largest bladed turbine shook violently during testing. This shows that at high wind speeds, turbines with larger blades are unstable. This may reduce the performance of the turbine, and it may break down.
- It can be concluded that the C-section vertical axis wind turbine is capable of producing electricity power even with low wind velocity for domestic used.

7.2 **Future Work**

In order to make some improvement in the performances of the Savonius wind turbine rotor, there are some recommended actions that could be done to further improve the results calculated from this study:

- The materials of Savonius wind turbine blade rotors should be improved by using some lighter materials and more durable so that it could be able to withstand any high pressures caused by the wind for some period of time.
- Further research will aim at developing and optimizing the Savonius wind turbine under static, dynamic and fatigue conditions. Also, the parameters of Savonius wind turbine rotor will be fully analyzed to enhance its effectiveness.

REFERENCES

ldo, V. (2009). *Fundamentals of Renewable Energy Processes.* Elsevier Inc., Unite State of America.

Ali, H. M. (2013). Experimental Comparison Study for Savonius Wind Turbine of Two and Three Blades at Low Wind Speed. *International Journal of Modern Engineering Research.*

Balachandran, P. (2011). *Engineering Fluid Mechanics.* PHI Leaming Private Limited, New Delhi.

Bhadra, S., N., Kastha, D., and Banerjee, S. (2005). *WindElectrical Systems.* Oxford University Press, India.

Bhaumik T. and Gupta R. (2010). Performance measurement of a two-bladed helical savonius rotor. *In Proceedings of the 37th National & 4th International Conference on Fluid Mechanics and Fluid Power* (pp. 74-77). Chennai IIT: Madras.

Biswas, A., Gupta, R., and Sharma, K. (2007). Experimental Investigation of Overlap and Blockage. *WindEngineering,* doi: http://dx.doi.org/10.1260/030952407783418702

Brunell, Dr. (2009). Students Harness Wind Energy, Stevens Institute/ of Technology. Retrieved June 11, 2015 from http://web.stevens.edu/green/infrastructure/campus.html

Busby, R. L. (2012). *Wind turbine design equations-from WindPower: The Industry Grows Up.* PenWell Corporation, Oklohama.

Can, K., Feng, Z., and Xuejun, M. (2010). Comparison Study of a Vertical-Axis Spiral Rotor and a Conventional Savonius Rotor". *In Power and Energy Engineering Conference (APPEEC)* (pp. 1-4), doi:10.1109/APPEEC.2010.5448791

Carrigan, T. J., Dennis, B. H., Han, Z. X., and Wang, B. P. (2012). Aerodynamic Shape Optimization of a Vertical-Axis Wind Turbine Using Differential Evolution. *International Scholarly Research Network ISRN Renewable Energy,* doi: http://dx.doi.org/10.5402/2012/528418

Choudhury, B., and Saraf, G. (2014). Computational Analysis of Flow around a Two-Bladed _,~oniusRotor, *isescojournal ofScience and Technology, 17 (1), 39-48.*

Diaz, F., Gavalda, J., and Massons, J., (1991). Drag and lift coefficient of the savonius wind machine, *Journal of WindEnergy, 4 (1), 240-246.*

Fox, R., and Mcdonald, A., and Pritchard, P. (2002). *Introduction to Fluid Mechanics.* New York: Wiley.

Gad, H., E., Abd El-Hamid, A. A., El-Askary, Q. A., and Nasef, M. H. (2014). A New Design of Savonius Wind Turbine: Numerical Study. *CFDLetters,* 6(4), 144-58.

Ghatage, S. V., and Jyeshtharaj B. J. (2011). Optimisation of Vertical Axis Wind Turbine: CFD Simulations and Experimental Measurements. *The Canadian Journal of Chemical Engineering.*

Ghosh, P., Kamoji, M.A., Kedare, S. B., and Prabhu, S. V. (2009) Model Testing of Single and Three-stage Modified Savonius Rotors and Viability Study of Modified Savonius Pump Rotor Systems. *International Journal of GreenEnergy,* 6(3), 22-41.

Graebel, W. P. (2001). *Engineeringfluid mechanics.* New York: Taylor & Francis.

Gupta, R., Das, R. Gautam, R., and S.S. Deka. (2012). CFD Analysis of a Two bucket Savonius Rotor for Various Overlap Conditions. *isesco Journal of Science and Technology, 8(13),* 67-74.

GWEC, Global Wind Energy Council. (2006). *Global wind 2006 report.* Gloval Wind Energy Council. Retrieved from http://gwec.net/wp-content/uploads/2012/06/ gwec-2006_final_01.pdf.

Hayashi, T., Yan L., and Yutaka Hara., (2005). Wind Tunnel Tests on a Different Phase Three Stage Savonius Rotor. *JSME International Journal,* 48(1), 332-343.

Hemami, A. (2012). *Windturbine technology.* Clifton Park, NY: Delmar, Cengage Leaming.

Hu, G., Li4, W., Xu, Zheng, Y., and Zhenzhou X. Z.. (2009). Research on the Improvement of tie' Performance of Savonius Rotor Based on Numerical Study. *In Sustainable Power Generation and Supply (SUPERGEN) '09,* doi: 10.1109/SUPERGEN.2009.5348197

IEA, (2002). *Key Word Energy Statistics.* Greece: IEA. Retrieved from http://www.env-edu.gr/Documents/Key%20Wor1d%20Energy%20Statistics%202006.pdf

Jamieson, P. (2011). Rotor Aerodynamic Design. In *Innovation in Wind Turbine Design* , doi: 10.1002/9781119975441.chl

Jeon, K. S Jeong, J., Pan J. I., and Ryu, K. (2015). Effects of end plates with various shapes and sizes on helical Savonius wind turbines. *Renewable Energy,* 79(4), 167-176.

Kacprazak, K., Liskiewicz G., and Sobczak, K. (2013). Numerical investigation of conventional and modified Savinous wind turbine. *Renewable Energy,* 60 (5), 578-585.

Kadam, A. A., and Patil, S. S. (2013). A Review on Savonius Wind Rotors for Accessing the Power Performance. *Journal of Mechanical and Civil Engineering,* 5, 18-24.

Kaldellis, J. K. (2010). *Stand-alone and hybrid wind energy systems: Technology, energy storage and applications.* Boca Raton, Fla.: CRC Press.

Kamoji, M. A., Kedare, S. B., and Pradhu, S. V. (2008). Experimental Investigation on the effect of overlap ration and blade edge conditions on the performance of conventional Savonius rotor. *Wind Engineering,* 32(6), 163-178.

Kamoji, M.A., Kedare, S. B., and Prabhu S. V. (2009). Performance tests on helical Savonius rotor. *Renewable Energy,* 34 (12), 521-529.

Kawamura T., Hayashi T., and Miyashita K. (2001). Application of the domain decomposition method to the flow around the Savonius rotor. *In 12th International Conference on Domain Decomposition Methods,* (pp.393-400). Chiba: Japan.

Kothari, D. P., Ranjan, R., and Singal, G. C. (2008). *Renewable Energy Sources and Emerging Technologies.* PHI, New Delhi.

Kumar, K. }·, and Prabhuraj, M. (2014). Fuzzy Logic Control Strategy for Stand-Alone Self-Excited Induction Generator for a Variable Speed Wind Turbine. *International Conference on Engineering Technology and Science-(ICETS'l4), International Journal of Innovative Research in Science, Engineering and Technology,* 3(7), 846-852.

Kumbemuss, J., Chen, H., Yang, H. X., and Lu., L. (2012). Investigation into the relationship of the overlap ratio and shift angle of double stage three bladed vertical axis wind turbine (VAWT). *Journal of Wind Engineering and Industrial Aerodynamics,* doi: 1O.1016/j.jweia.2012.03.021

Manzoor, H. M., Mehdi, S. N., and Reddy, P.R., (2008). CFD Analysis of Low Speed Vertical Axis Wind. *International Journal of Applied Engineering Research,* 3(1),149-159.

Morshed, K. N. (2010). *Experimental and numerical investigations on aerodynamic characteristics of Savonius wind turbine with various overlap ratios* (master thesis). Georgia Southern University, Statesboro, Georgia.

Norhazwani, (2014). *Comparison Performance among Micro-Size of Vertical Axis Wind Turbines.* Universiti Teknologi Malaysia, Malasia

Patibandla, N. (2008). *Clean and Renewable Energy Opportunities* (doctoral dissertation). Center for Future Energy Systems Rensselaer Polytechnic Institute, Troy, New York.

Qasim, A. Y., Usubamatov, R., and Zain, Z. M.(2011). Investigation and Design Impeller Type Vertical Axis Wind Turbine." *Australian Journal of Basic and Applied Sciences, 5(12), 121-126.*

Ravichandrudu, K., and Kumar, P. S. (2014). Power Quality Improvement For Grid Connected Wind Energy System By Using Statcom. *International Journal of Application or Innovation in Engineering & Management,* 3(9), 2014

Rahman, M., Morshed, K. J., Lewis, J. and Fuller, M. (2009). Experimental and numerical investigations of drag and torque characteristics of three-bladed Savonius wind turbine. *In Proceedings of the ASME 2009 International Mechanical Engineering Congress & Exposition,* (pp. 85-94). Lake Buena Vista: Florida.

Saha, U., at Rajkumar, M. (2006). On the performance analysis of Savonius rotor with twisted bledes. *Renewable Energy, 31(11), 1776-1788.*

Saha, U. K., Thotla, S., and Maity, D., (2008). Optimum design configuration of Savonius rotor through wind tunnel experiments." *Journal of Wind Engineering and Industrial Aerodynamics,* doi: 1O.1O16/j .jweia.2008. 03.005

Sargolzaei, J. (2007). Prediction of the power ratio and torque in wind turbine Savonius rotors using artificial neural networks. *In Proceedings of the WSEAS International Conference on Renewable Energy Sources,* (7-12). Arcachon: France

Shashank, P., Walter, F., Brien, O., and Danesh, K. (2013). Small-scale Wind Energy Portable Turbine (SWEPT) (master thesis). Virginia Polytechnic Institute and State University, United States of America.

Shepherd, G., (1990). *Historical Development of the windmill.* National Aeronautics and Space Administration, Contractor Report 4337 DOE/NASA/5266-1). Ithaca, New York: Cornell University.

Singh, G. (2008). *Exploit Nature-Renewable Energy Technologies.* Aditya Books Pvt. Ltd., New Delhi.

Sullivan, A. (2010). *Aerodynamic forces acting on an airfoil, Physics Department;* The College of Wooster; Wooster, Ohio.

Telles , M. (2006). *Wind Energy: Technology; Commercial Projects and Laws.* Nova Science Publisher, New York.

Wenehenubun, F., Saputra, A., and Hadi S. (2015). An experimental study on the performance of Savonius wind turbines related with the number of the blades. *In 2nd international conference on sustainable energy engineering and Application Sustainable Energy for Green Mobility, 68(9), 297-304.*

Wulff, H. E. (1967). *The traditional crafts of Persia, their development, technology and influence on eastern and western civilization.* M.I.T. Press, Cambridge.